AD-A087 478 HARRIS SAI INC ANN ARBOR MI F/G 20/14
VARIATIONAL ANALYSIS OF HELICAL SLOW WAVE STRUCTURES.(U)
MAY 80 T P FONTANA, D M MACGREGOR F30602-79-C-0013
UNCLASSIFIED RADC-TR-80-174 NL

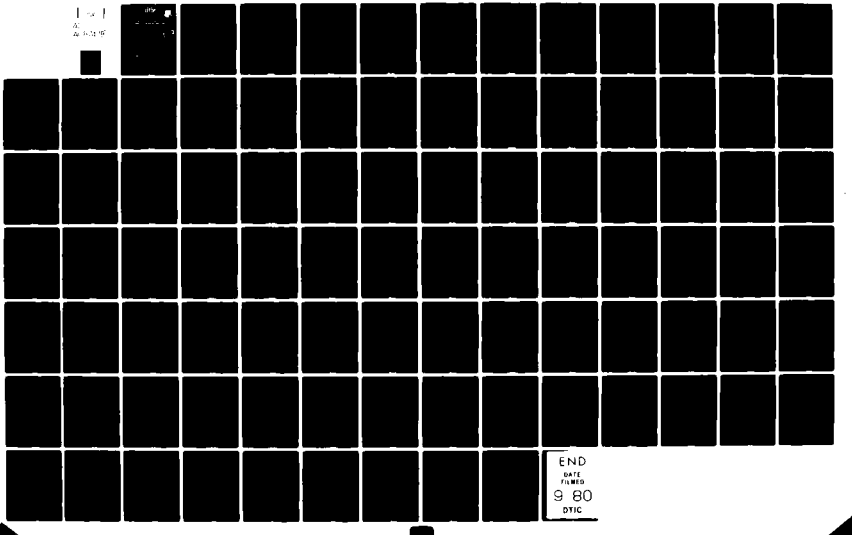

END
DATE FILMED
9 80
DTIC

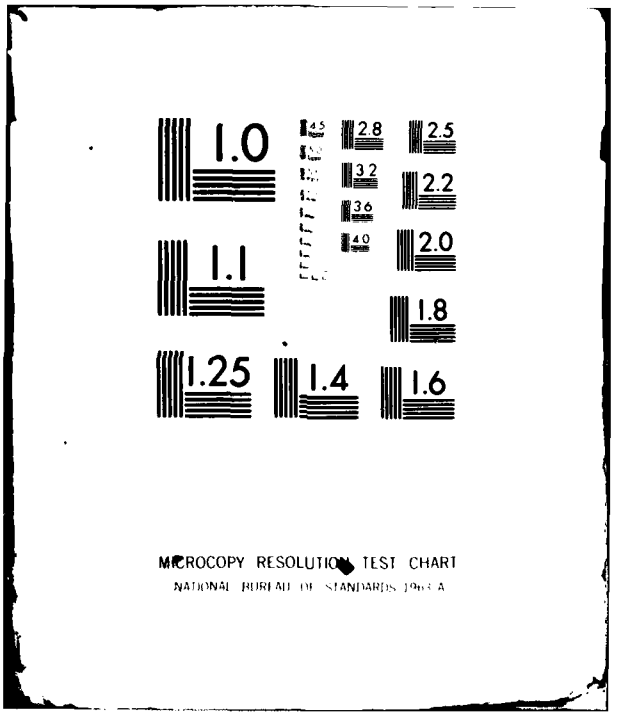
1.0
1.1
1.25
1.4
1.6
1.8
2.0
2.2
2.5
2.8
3.2
3.6
4.0
MICROCOPY RESOLUTION TEST CHART
NATIONAL BUREAU OF STANDARDS 1963 A

RADC-TR-80-174
Final Technical Report
May 1980

LEVEL F

12

VARIATIONAL ANALYSIS OF HELICAL SLOW WAVE STRUCTURES

Harris SAI, Incorporated

Dr. T. P. Fontana
Dr. D. M. MacGregor

ROME AIR DEVELOPMENT CENTER
Air Force Systems Command
Griffiss Air Force Base, New York 13441

This report has been reviewed by the [illegible] and is releasable to the National Technical Information [illegible] At NTIS it will be releasable to the general public, [illegible] nationals.

RADC-TR-80-174 has been reviewed and is approving for publication.

APPROVED: Joseph J. Polniaszek

JOSEPH J. POLNIASZEK
Project Engineer

APPROVED: Frank J. Rehm

FRANK J. REHM
Technical Director
Surveillance Division

FOR THE COMMANDER: John P. Huss

JOHN P. HUSS
Acting Chief, Plans Office

If your address has changed or if you wish to be removed from the RADC mailing list, or if the addressee is no longer employed by your organization, please notify RADC (OCTP), Griffiss AFB NY 13441. This will assist us in maintaining a current mailing list.

Do not return this copy. Retain or destroy.

UNCLASSIFIED

SECURITY CLASSIFICATION OF THIS PAGE (When Data Entered)

REPORT DOCUMENTATION PAGE	READ INSTRUCTIONS BEFORE COMPLETING FORM
1. REPORT NUMBER: RADC-TR-80-174	2. GOVT ACCESSION NO.: AD-A087478	3. RECIPIENT'S CATALOG NUMBER
4. TITLE (and Subtitle): VARIATIONAL ANALYSIS OF HELICAL SLOW WAVE STRUCTURES.	5. TYPE OF REPORT & PERIOD COVERED: Final Technical Report. 25 Oct 78 — 24 Jan 80
	6. PERFORMING ORG. REPORT NUMBER: N/A
7. AUTHOR(s): T. P. Fontana, D. M. MacGregor	8. CONTRACT OR GRANT NUMBER(s): F30602-79-C-0013
9. PERFORMING ORGANIZATION NAME AND ADDRESS: Harris SAI, Incorporated, 611 Church Street, Ann Arbor MI 48104	10. PROGRAM ELEMENT, PROJECT, TASK AREA & WORK UNIT NUMBERS: 62702F, 45061233
11. CONTROLLING OFFICE NAME AND ADDRESS: Rome Air Development Center (OCTP), Griffiss AFB NY 13441	12. REPORT DATE: May 1980; 13. NUMBER OF PAGES: 91
14. MONITORING AGENCY NAME & ADDRESS (if different from Controlling Office): Same	15. SECURITY CLASS. (of this report): UNCLASSIFIED; 15a. DECLASSIFICATION/DOWNGRADING SCHEDULE: N/A

16. DISTRIBUTION STATEMENT (of this Report)

Approved for public release; distribution unlimited.

17. DISTRIBUTION STATEMENT (of the abstract entered in Block 20, if different from Report)

Same

18. SUPPLEMENTARY NOTES

RADC Project Engineer: Joseph J. Polniaszek (OCTP)

19. KEY WORDS (Continue on reverse side if necessary and identify by block number)

Variational	TWT
Cold test	Dispersion
Helix	Interaction impedance
Composite metal-ceramic	

20. ABSTRACT (Continue on reverse side if necessary and identify by block number)

A variational technique has been used in predicting impedance and dispersion characteristics for the cold test measurements of helical traveling wave tubes. The variational formula of Bevensee is used in this method. An optimal combination of slow wave trial fields is found using Rumsey's reaction integral as a measure of equivalence to the true fields. In contrast to other approximate analyses, the variational formulation has the advantage of including the exact geometry and (Cont'd)

DD FORM 1 JAN 73 1473 EDITION OF 1 NOV 65 IS OBSOLETE

UNCLASSIFIED

SECURITY CLASSIFICATION OF THIS PAGE (When Data Entered)

394541

Item 20 (Cont'd)

dielectric of the helical support.

In order to verify the technique, two trial field regions have been used in successfully analyzing the sheath helix and the case of a homogeneous dielectric support. A composite metal-ceramic helix has also been analyzed. Simulation for the composite helix shows a reasonable dispersion for some combinations of harmonics over a wide frequency range when results are compared to experiment. However, the impedance computation is not yet satisfactory.

In future developments, major modifications will be made to the trial fields in order to satisfy all boundary conditions simultaneously and improve the predicted impedance. In addition, the technique will be applied to other devices including wedge and rod supports.

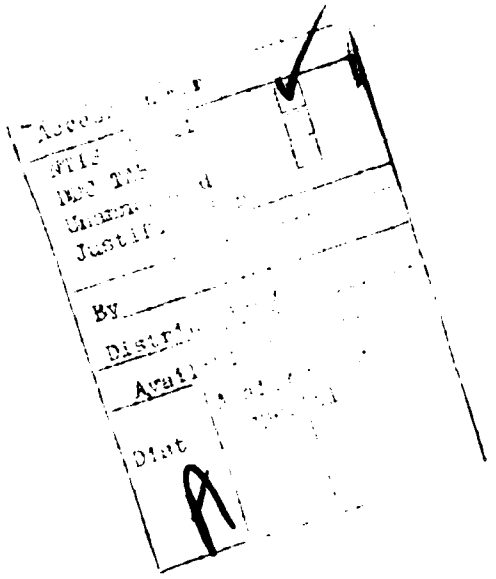

TABLE OF CONTENTS

		Page
I.	INTRODUCTION	1
II.	RESEARCH OBJECTIVES	2
III.	VARIATIONAL TECHNIQUE	8
	A. Assumptions	8
	B. Notation	9
	C. Boundary Conditions and Trial Fields	12
	D. Bevensee's Variational Formula	14
	E. Reaction Method	18
	F. Variational Nature of the Reaction Integral	22
	G. Symmetric Properties from Reaction	23
IV.	COMPUTATIONAL RESULTS FOR THE VARIATIONAL ANALYSIS OF A SHEATH HELIX	24
V.	VARIATIONAL ANALYSIS OF A HELICAL TAPE SUPPORTED BY AN HOMOGENEOUS DIELECTRIC REGION	26
	A. Four Coefficients Per Angular Harmonic	26
	B. Spurious Propagation Constants	31
	C. Use of Reaction Method to Generate a New Convergent Variational Expression	31
	D. Continuity Constraints at the Trial Field Interface	32
	E. Use of Constraints to Obtain Convergent Results for Impedance and Dispersion	38
VI.	VARIATIONAL ANALYSIS OF A SPIRAL DIELECTRIC SUPPORT	49
	A. Two Trial Field Regions	49
	B. Three Region Problems	51
	C. Numerical Difficulties in Three Region Ceramic-Coated Helix Problems	62
VII.	ERRORS INTRODUCED BY BEVENSEE'S CHOICE OF THE TRIAL FIELD	68

TABLE OF CONTENTS (concluded)

		Page
VIII.	SUGGESTIONS FOR FUTURE WORK	71
	A. Alternate Trial Fields	71
	B. Reduction of Trial Field Harmonics by Point Matching	72
	C. Use of Other Variational Expressions on the Spiral Dielectric	73
IX.	CONCLUSIONS	74
REFERENCES		76
APPENDIX A:	DATA FOR A NORTHROP CORPORATION METAL-CERAMIC TAPE HELIX	78

LIST OF ILLUSTRATIONS

Figure		Page
1	The Tape Helix	3
2	Two Methods of Supporting a Helix	4
3	Vane-Loaded Helix	5
4	Supports Analyzed a. Homogeneous Dielectric Sleeve b. Composite Metal-Ceramic Helix	6
5	Wedge Dielectric Support Showing Volume and Surface Notation	10
6	Spiral-Dielectric Support Showing Volume and Surface Conventions	11
7	Comparison Between the Exact Dispersion Solution for the Sheath Helix and that Found by the Variational Method	25
8	Comparison Between Impedance at the Tape From Paik Theory and Variational Method for Helix No. 2 Without Dielectric	28
9	Comparison Between Phase Velocities From Paik Theory and Variational Method for Composite Helix No. 2 Without Dielectric	29
10	Cancelling Additional Currents Across the Interface of Trial Field Regions	33
11	Tangential E Boundary Values at Tape Radius Using Five Harmonics	34
12	Tangential E Boundary Values at Tape Radius Using Seven Harmonics	35
13	Tangential E Boundary Values at Tape Radius Using 11 Harmonics	36
14	Comparison Using 23 Harmonics Between Impedances at the Tape from Variational Method and Paik Theory Applied to Helix No. 2 Without Dielectric	43

LIST OF ILLUSTRATIONS (cont'd.)

Figure		Page
15	Comparison Using 23 Harmonics Between Phase Velocities From Variational Method and Paik Theory Applied to Helix No. 2 Without Dielectric	44
16	Comparison Using 23 Harmonics Between Impedance at the Tape from Variational Method and Paik Theory Applied to Helix No. 2 With Mean Dielectric	45
17	Comparison Using 23 Harmonics Between Phase Velocities from Variational Method and Paik Theory Applied to Helix No. 2 with Mean Dielectric	46
18	CPU Time in Three Trial Region Spiral Dielectric Variational Analysis as the Number of Harmonics Increases	53
19	Trends in Line Impedance Phase Velocity as the Number of Trial Fields Increases on Composite Helix No. 2	54
20	Trends in Line Impedance and Phase Velocity when Some Harmonics are Deleted and Simulation for Composite Helix No. 2	55
21	Comparisons Between Phase Velocities From Variational Method, Paik Theory and Experiment for Composite Metal Ceramic Helix No. 2	57
22	Trends in Phase Velocity vs. the Number of Trial Field Harmonics in Simulation of Hughes Composite Helix	58
23	Comparison of Phase Velocity from Variational Method, Paik Theory and Experiment for Hughes Composite Metal Ceramic Helix	59
24	Comparison Among Phase Velocities for Hughes Ceramic Helix Using 23 Harmonics	60

LIST OF ILLUSTRATIONS (concluded)

Figure		Page
25	Comparison of Dielectric Loading Effects From Simulation and Measurements for Hughes Metal-Ceramic Helix	61
26	Comparison of Shield Loading Effects from Simulation and Measurement for Hughes Metal Ceramic Helix	63
27	Comparison of Phase Velocities from Variational Analysis, Paik Theory and Experiment for Composite Helix No. 1	64
28	Comparison of Phase Velocities from Variational Analysis, Paik Theory and Experiment for Composite Helix No. 3	65

LIST OF TABLES

		Page
1	Phase Velocity and Impedance for Helix No. 4 Without Dielectric at 6 GHz Using Four Trial Fields Per Harmonic	30
2	Trends Using New Variational Expression on Composite Helix No. 2 Without Dielectric	37
3	Helix No. 2 Without Dielectric Gap/Pitch = .35	39
4	Helix No. 2 With Dielectric Gap/Pitch = .35	40
5	Helix No. 1 Without Dielectric Gap/Pitch = .49	41
6	Helix No. 4 Without Dielectric Gap/Pitch = .77	42

EVALUATION

A significant cost associated with the design and development of helical traveling wave tubes has been incurred by "cut and try" techniques. Various analytic methods have been developed to attempt to adequately model a slow wave structure,however, these at best have been first order approximations. The variational technique described herein and implemented on the RADC GCOS computer is a large deviation from present "lumped" models. Although not completely refined, the variational technique promises to deliver an order of magnitude improvement in helical structure modeling without resorting to "correction factors"that are structural type dependent. Therefore, in tube design, it may be possible using the variational computer software to completely design a workable structure in one or two hardware iterations.

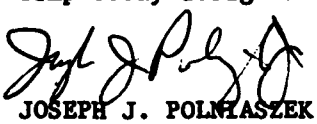

JOSEPH J. POLNIASZEK
Project Engineer

SECTION I

INTRODUCTION

In November 1979,Harris SAI, Inc., Ann Arbor, Michigan began the development of computer programs for variational analysis of helical slow-wave structures for O-type traveling-wave tubes. The basic objective was to develop more accurate computer models than were previously available for the computation of dispersion, impedance and attenuation and thereby minimize the cold testing needed for development of new TWT designs.

This Final Technical Report describes the progress in the development and application of the variational technique achieved under the contract. Section II describes the objectives of this research effort. Section III presents the methodology of the techniques developed. Numerical results for the sheath helix are summarized in Section IV. The analysis on an homogeneous dielectric support is detailed in Section V. Work done on the spiral dielectric structure and comparisons between simulation and cold test data are found in Section VI. The consequences of Bevensee's choice of trial fields is examined in Section VII, and alternate trial fields are proposed for future work in Section VIII. Conclusions are presented in Section IX.

This effort was supported by Rome Air Development Center, Griffiss AFB, New York under Contract No. F30602-79-C-0013.

SECTION II

RESEARCH OBJECTIVES

In helical traveling-wave tubes, the slow-wave circuit is commonly supported inside a vacuum envelope by means of dielectric rods, wedges, or more recently by a ceramic coating deposited upon the helical tape. These geometries are illustrated in Figures 1 through 4. It is known from experiments that these supports increase the dispersion and lower the interaction impedance. Also, in some designs longitudinal vanes or other configurations are inserted inside a conducting shield to reduce dispersion and taper phase velocity.

In a typical tube development, the slow wave structure is designed using approximate theories and then is cold tested experimentally because no accurate theoretical predictions of dispersion and impedance have been available. This can be attributed to the necessary approximations used in the popular non-variational, analytic techniques. For example, the conducting tape helix is often modeled as a spiralling conducting sheath[1,2] or else a particular current distribution is assumed over the metal surface.[3,4] Moreover, existing theories of dielectric loading have treated the dielectric supports, no matter what their shape, as filling the entire region between the helix and shield.[2,5] Usually the effective dielectric constant either is adjusted phenomologically or else is scaled by the proportion of volumes occupied by the support. A more rigorous treatment states the boundary condition in full but uses approximate radial propagation constants in the dielectric and vacuum to obtain analytic results.[6] Vane loading has been treated by an equivalent transmission-line

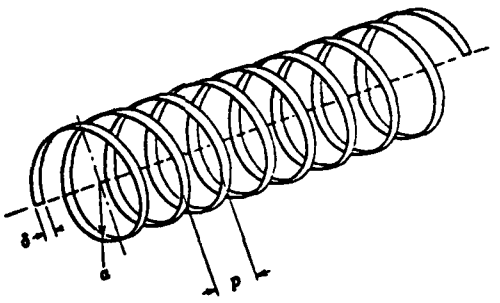

Figure 1. The tape helix.

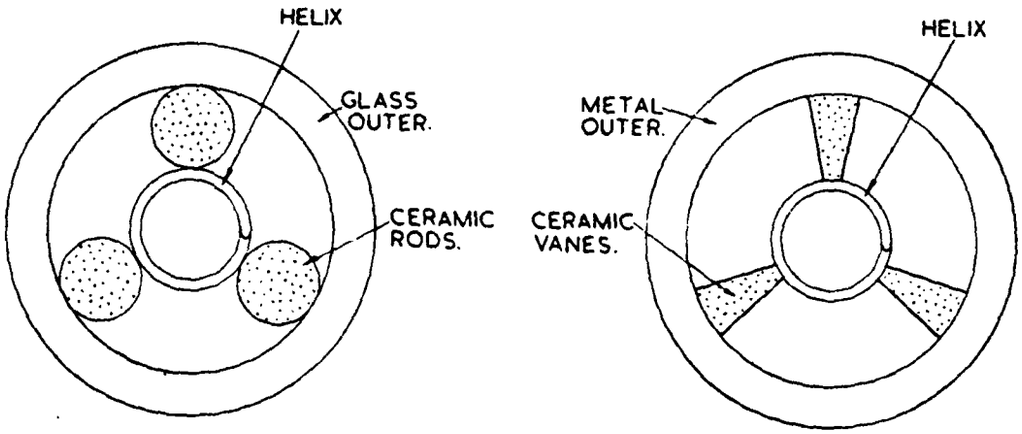

Figure 2. Two methods of supporting a helix.

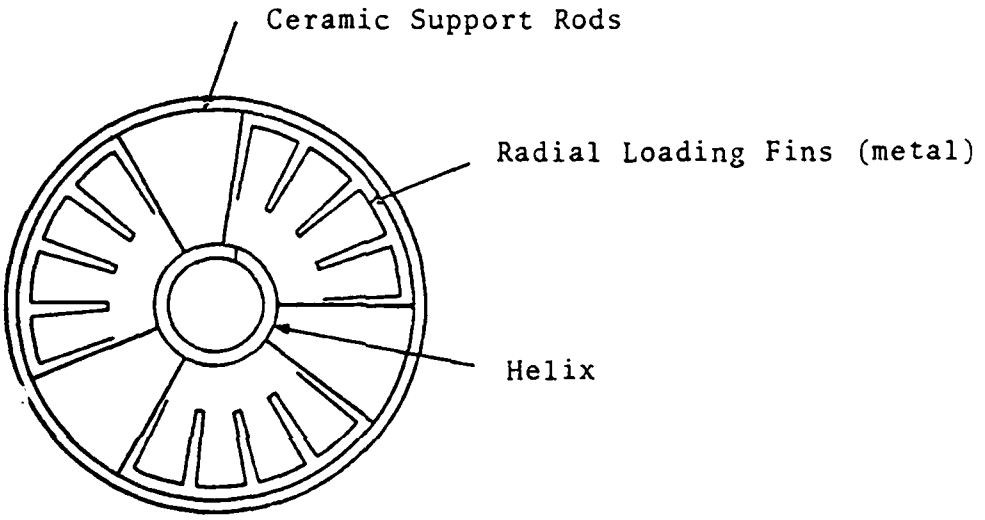

Figure 3. Vane-loaded helix.

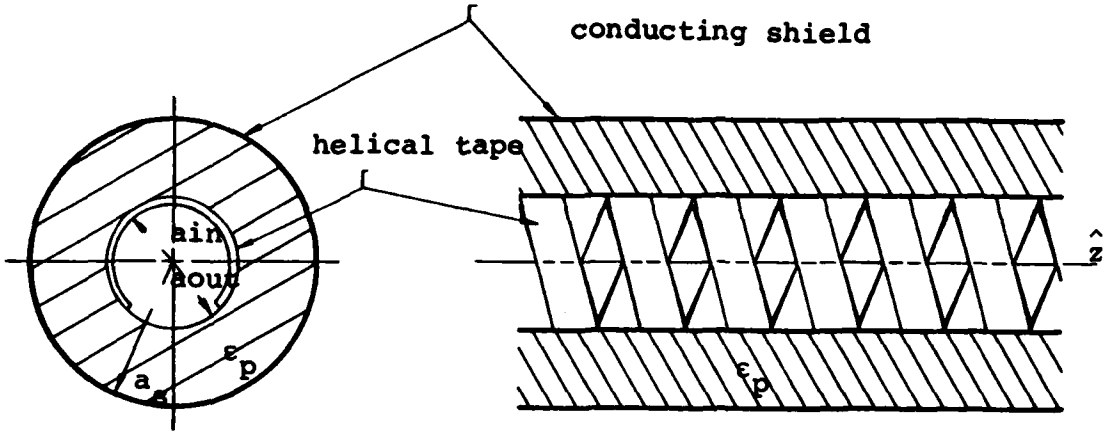

a) Homogeneous dielectric sleeve

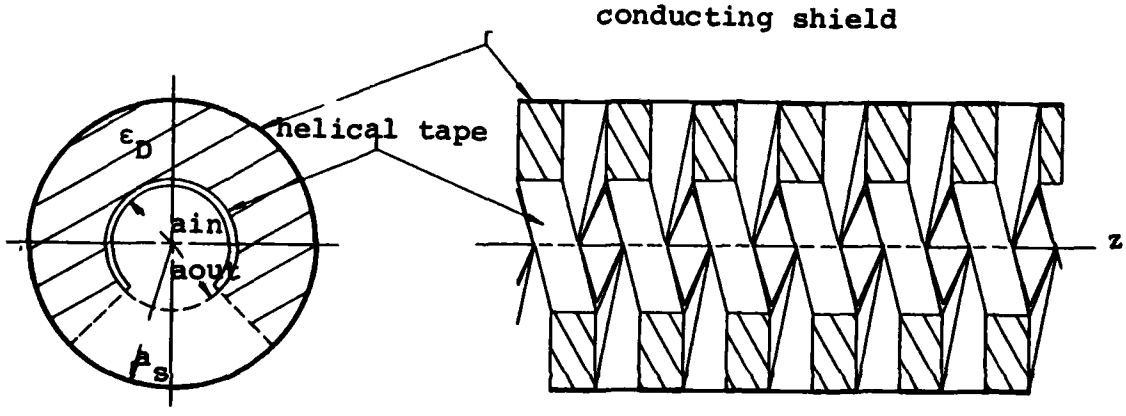

b) Composite metal-ceramic helix

Figure 4. Supports analyzed.

method,[5] but the theory assumes only a single space narmonic.

During this contract, Harris SAI, Inc. began adapting the variational technique of Bevensee[7] to treat various dielectric-supported slow-wave structures. Unlike other techniques, the actual geometry and dielectric of the structures is used. The main objectives of the work are to (1) develop an accurate computational analysis of supported, helix-type structures and (2) verify the theory using existing cold-test data.

The structures originally selected for study under this contract were sheath helices, and radially thin tape helices supported in metal shields by a homogeneous dielectric region, a spiralling dielectric, rods, or wedges which may be asymetrically placed. Of these configurations, the analyses for the sheath helix and tape helices supported by homogeneous and spiral dielectric were fully developed. The latter case had its true, radial tape thickness modeled so that all structural dimensions were employed in the analysis.

The analysis of the sheath helix was included so that the computer program could be verified. The homogeneous support structure is a typical approximation used in analyzing complicated devices. Comparisons between the variational analysis and Paik theory are presented because the Paik theory also makes this approximation of an homogeneous external region. The particular computer program referenced in this report as Paik is based upon theory developed by Watkins,[2] Ash,[8] and Paik.[5] It is part of the Harris SAI's TWA small-signal group of programs[9] for which it estimates cold test data. The results from the spiral dielectric support were compared with both the Paik theory and experimental cold test data.

SECTION III

VARIATIONAL TECHNIQUE

The objective of the variational technique is to combine trial cylindrical electric and magnetic fields in a manner that appropriately satisfies all boundary conditions. A variational formula given by Bevensee[7] is used because it allows the derivation of the dispersion relation prior to the calculation of trial field coefficients. In this section, the principal assumptions of the model are presented. Trial fields and boundary conditions are developed, and Bevensee's variational expression is introduced. This formula is shown to be actually a specific application of the reaction concept developed by Rumsey[10] which uses Bevensee's trial fields and boundary conditions. From the reaction concept, alternate variational forms are developed, symmetric properties of these expressions are shown, and convergence is examined.

A. Assumptions

In the computational analyses the slow-wave structure is modeled as follows:

(1) The slow-wave structure is assumed to be infinite in length with fixed period. Thus, end effects are neglected and a tapered helix is treated as if its local pitch is constant.

(2) The effect of skin loss is sufficiently small that the fields within the metal are negligible and the surface boundary conditions for a perfectly conducting surface apply. This makes the fields and propagation constants independent of the conductivity.

(3) The metal and dielectric surfaces are perfectly smooth and unperturbed throughout the structure.

(4) The dielectric material is uniform, isotropic and lossless.

(5) The magnetic permeability has the free space value, denoted μ_0.

(6) Perfect contact exists at any dielectric-metal interface.

B. Notation

All electric and magnetic fields have the exp(jwt) time convention where $\omega = 2\pi x$ frequency. References will be made to particular dimensions of the slow-wave structure. Figures 5 and 6 illustrate the various volumes and surfaces. The following definitions are convenient.

Divide the single period of the slow wave structure into three volume regions as follows:

V_i free space within the helix;

V_o free space outside the helix;

V_d dielectric volume.

Define the surfaces of the region interfaces as follows:

W_i inner wire surface;

W_o outer wire surface bounded by free space;

W_d outer wire surface bounded by dielectric material;

D_o interface of regions V_i and V_o at helix radius (interior and exterior free space regions);

D_d interface of regions V_i and V_d at helix radius (interior free space and dielectric regions);

A transverse dielectric boundary (extending radially outwards from the helix radius).

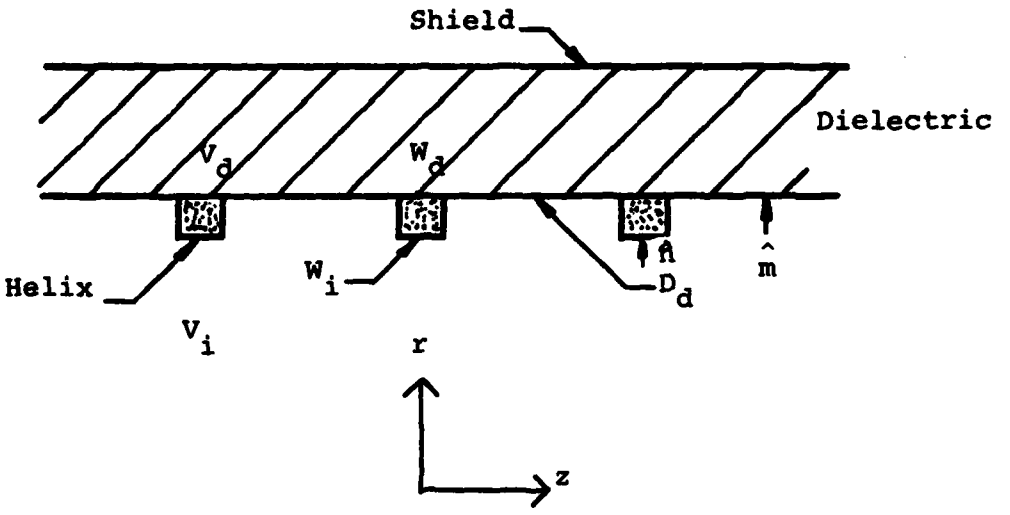

a. Longitudinal section

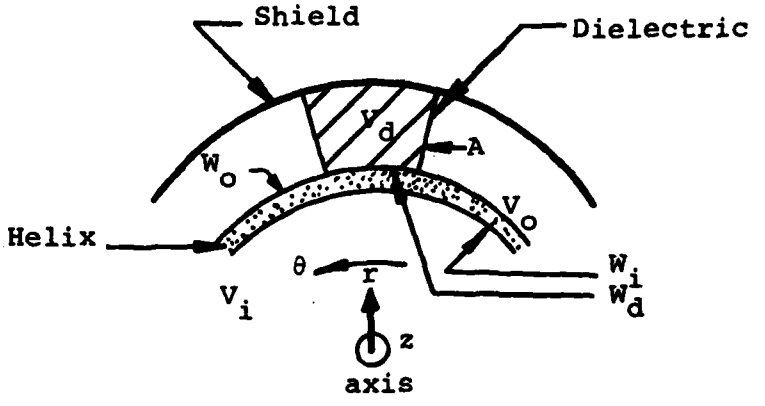

b. Transverse section

Figure 5. Wedge dielectric support showing volume and surface notation.

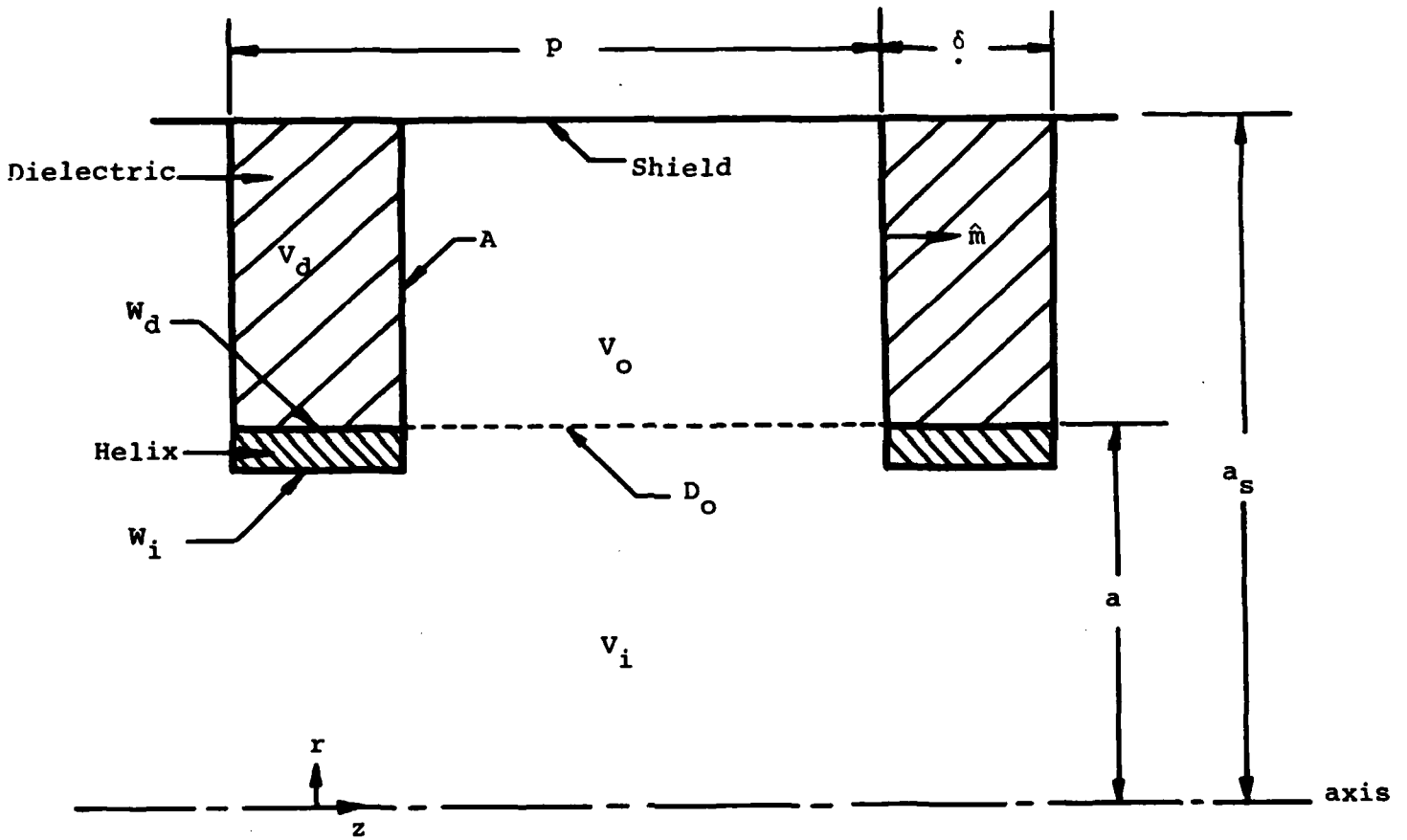

Figure 6. Spiral-Dielectric support showing volume and surface conventions.

Let the helix have pitch angle ψ and radius a. Let the shield have radius a_s.

Cylindrical coordinates (r, θ, Z) are used throughout this report. The following unit vectors will be used:

$\hat{r}$ outward normal;

$\hat{n}$ normal into helical surface, which is $\pm \hat{r}$ for a thin tape helix;

$\hat{t}$ normal to helix surface and $\hat{r}$ or (0, -sin ψ, cos ψ) in cylindrical coordinates;

$\hat{m}$ into the dielectric and normal to the surface.

C. Boundary Conditions and Trial Fields

Currently, two types of slow-wave structures have been successfully analyzed. Each has a helically-wrapped conducting tape supported within a shield. The support of each structure is periodic. One support is just an isotropic homogeneous dielectric placed between the tape and the shield (see Figure 4a). The second is a composite metal ceramic structure, meaning that the isotropic dielectric has been deposited on top of the tape giving a spiralling dielectric support (see Figure 4b).

The correct fields must satisfy Maxwell's equations, have periodic properties, and satisfy the correct boundary conditions at all surfaces.

The variational formulas produce best results when the trial solutions are close to the correct solution. Bevensee expresses his trial functions in cylindrical geometry. If the longitudinal axis of a tube is in the $\hat{Z}$ direction the periodicity of the true field implies that the propagating field must be a sum of cylindrical harmonics with phase

$$\Phi_n = -\beta_0 Z + n(\theta - \frac{2\pi}{\rho} Z) \quad , \tag{1}$$

where p is the period of the wrapping along Z. If the radial dependence is denoted $\vec{R}_{nm}(r)$ for each harmonic, the complete field is

$$\vec{F} = \sum_{m} \sum_{n} \vec{R}_{nm}(r) \; e^{j\Phi n} \quad . \tag{2}$$

Equation 1 makes the phase such that the field is invariant parallel to the helical tape except for propagation $\exp(-j\beta_0 Z)$. This β_0 is the fundamental propagation constant and one of the main quantities that the variational technique calculates. Bevensee forced each term of Equation 2 to satisfy Maxwell's equations. Then n=m and each component of $\vec{R}_n$ is a linear combination of modified Bessel functions of order n denoted $I_n(\gamma_n r)$, $K_n(\gamma_n r)$. Here

$$\gamma_n^2 = \beta_n^2 - k^2 \tag{3}$$

is the radial propagation constant where

$$\beta_n = \beta_0 + \frac{2\pi}{p} n \tag{4}$$

and k is the wave number of the space.

Although individually for each harmonic n, Bevensee's trial fields have the correct phase and satisfy Maxwell's equations, they do not satisfy boundary conditions. Bevensee tries to piece together a satisfactory solution. First, he partitions the structure into regions V_i, V_o, V_D defined earlier. For each harmonic, n, the inner region, V_i, has a TE and TM set of fields written as an I-type Bessel function.

Simultaneously, each outer region has TE and TM sets dependent upon a linear combination of I and K-type Bessel functions such that the boundary conditions at the shield are satisfied. Physically, these combinations give for each n an exponentially growing field for the inner region and an exponentially decaying field in the outer region. By considering all harmonics n, it is assumed that the boundary conditions at the helical tape, trial region interfaces and dielectric-free space interfaces can be satisfied through an optimal selection of TE and TM coefficients.

D. Bevensee's Variational Formula

The variational equation presented in this section applies for a wire or tape helix of arbitrary cross section wound on an arbitrary cylindrical surface. It is based on the work of Bevensee,[7] but includes also the third, dielectric, region outside the helix.

The electric and magnetic fields for all harmonics n in Equation 1 within each region are defined as follows:

in region V_i: $\vec{e}$ and $\vec{h}$;

in region V_o: $\vec{E}$ and $\vec{H}$;

in region V_D: $\vec{\mathcal{E}}$ and $\vec{\mathcal{H}}$.

The longitudinal components of the TE or TM field in each region are

$$h_z = e^{j\beta_0 z} \sum_{n=0}^{N} C_{1n} I_n(\gamma_n r) e^{jn\psi} \quad , \tag{5a}$$

$$e_z = e^{j\beta_0 z} \sum C_{2n} I_n(\gamma_n r) e^{jn\psi} \quad , \tag{5b}$$

$$H_z = e^{j\beta_0 z} \sum C_{3n} S_n(\gamma_n r) e^{jn\psi} \quad , \tag{6a}$$

$$E_z = e^{j\beta_0 z} \sum C_{4n} R_n(\gamma_n r) e^{jn\psi} \quad , \tag{6b}$$

$$E_z = e^{j\beta_0 z} \sum C_{5n} T_n(\hat{\gamma}_n r) e^{jn\psi} \quad , \tag{7a}$$

$$H_z = e^{j\beta_0 z} \sum C_{6n} U_n(\hat{\gamma}_{nr}) e^{jn\psi} \quad , \tag{7b}$$

where $\psi = \theta - \frac{2\pi}{p} z$, (8)

$$\gamma_n^2 = \beta_n^2 - k_0^2 \quad , \tag{9}$$

$$\hat{\gamma}_n^2 = \beta_n^2 - k_0^2 \epsilon_D \quad , \tag{10}$$

$$R_n = K_n(\gamma r) - \frac{K_n(\gamma a_s)}{I_n(\gamma a_s)} I_n(\gamma r) \quad , \tag{11}$$

$$S_n = K_n(\gamma r) - \frac{K_n'(\gamma a_s)}{I_n'(\gamma a_s)} I_n(\gamma r) \quad , \tag{12}$$

$$T_n = K_n(\hat{\gamma} r) - K_n(\hat{\gamma} a_s)/I_n(\hat{\gamma} a_s)\ I_n(\hat{\gamma} r) \quad , \tag{13}$$

$$U_n = K_n(\hat{\gamma} r) - K_n'(\hat{\gamma} a_s)/I_n'(\hat{\gamma} a_s)\ I_n(\hat{\gamma} r) \quad . \tag{14}$$

Provided that the interface exists in the particular helix structure considered, boundary conditions on the tangential field components at each volume interface become:

$$(\vec{e} - \vec{E}) \times \hat{r} = 0 \text{ or surface } D_0, \tag{15}$$

$$(\vec{h} - \vec{H}) \times \hat{r} = 0 \quad , \tag{16}$$

$$\vec{e} \times \hat{r} = 0 \text{ on } W_i \quad , \tag{17}$$

$$\vec{E} \times \hat{r} = 0 \text{ on } W_o \quad , \tag{18}$$

$$\vec{E} \times \hat{r} = 0 \text{ on } W_d \quad , \tag{19}$$

$$(\vec{e} - \vec{E}) \times \hat{r} = 0 \text{ on surface } D_d \quad , \tag{20}$$

$$(\vec{h} - \vec{H}) \times \hat{r} = 0 \text{ on surface } D_d \quad , \tag{21}$$

$$(\vec{E} - \vec{E}) \times \hat{t} = 0 \text{ on surface A} \quad , \tag{22}$$

$$(\vec{H} - \vec{H}) \times \hat{t} = 0 \text{ on surface A} \quad . \tag{23}$$

Bevensee has devised a formula dependent upon the boundary condition mismatch:

$$\begin{aligned}
0 = & \int_{V_i} \vec{e}^{*} \cdot (\nabla \times \vec{h}_{+} - j\omega\varepsilon_0 \vec{e}_{+}) dV - \int_{V_i} \vec{h}^{*} \cdot (\nabla \times \vec{e}_{+} + j\omega\mu_0 \vec{h}_{+}) dV \\
& + \int_{V_o} \vec{E}^{*} \cdot (\nabla \times \vec{H}_{+} - j\omega\varepsilon_0 \vec{E}_{+}) dV - \int_{V_o} \vec{H}^{*} \cdot (\nabla \times \vec{E}_{+} + j\omega\mu_0 \vec{H}_{+}) dV \\
& + \int_{V_d} \vec{E}^{*} \cdot (\nabla \times \vec{H}_{+} - j\omega\varepsilon_D \vec{E}_{+}) dV - \int_{V_d} \vec{H}^{*} \cdot (\nabla \times \vec{E}_{+} + j\omega\mu_0 \vec{H}_{+}) dV \\
& + \int_{W_i} \vec{e}_{+} \times \vec{h}^{*} \cdot \hat{n} dS + \int_{W_o} \vec{E}_{+} \times \vec{H}^{*} \cdot \hat{n} dS + \int_{W_d} \vec{E}_{+} \times \vec{H}^{*} \cdot \hat{n} dS \\
& + \frac{1}{2} \int_{D_o} (\vec{e}^{*} + \vec{E}^{*}) \times (\vec{h}_{+} - \vec{H}_{+}) \cdot \hat{r} \, dS + \frac{1}{2} \int_{D_o} (\vec{e}_{+} - \vec{E}_{+}) \times (\vec{h}^{*} + \vec{H}^{*}) \cdot \hat{r} \, dS \\
& + \frac{1}{2} \int_{D_d} (\vec{e}^{*} + \vec{E}^{*}) \times (\vec{h}_{+} - \vec{H}_{+}) \cdot \hat{r} \, dS + \frac{1}{2} \int_{D_d} (\vec{e}_{+} - \vec{E}_{+}) \times (\vec{h}^{*} + \vec{H}^{*}) \cdot \hat{r} \, dS \\
& + \frac{1}{2} \int_{A} (\vec{E}^{*} + \vec{E}^{*}) \times (\vec{H}_{+} - \vec{H}_{+}) \cdot \hat{m} dS \\
& + \frac{1}{2} \int_{A} (\vec{E}_{+} - \vec{E}_{+}) \times (\vec{H}^{*} + \vec{H}^{*}) \cdot \hat{m} dS \quad . \qquad (24)
\end{aligned}$$

The "+" fields in Equation 24 are the correct solution propagating in the z direction, while the "-" fields are a second set of fields propagating in the -z direction. Because the trial fields satisfy Maxwell's equations, the volume integrals are identically zero when the dielectric constant equals that of the trial fields throughout the trial field region.

This expression is variational in the sense that any arbitrary perturbation in the "-" fields for the correct "+" fields still yields a zero in expression (24) and vice versa. This characteristic is used to derive the field coefficients. Assuming that the field solution can be expressed as a sum of slow wave cylindrical harmonics within each trial region, Equation 24 becomes a quadratic form in terms of the "+" and "-" field coefficients

$$0 = B^{\dagger} M(\beta_0) C \ , \qquad (25)$$

where C is a column vector of all <u>true</u> coefficients in Equations 5 through 10 and B is the column vector of the "-" field coefficients. The † denotes conjugate transpose. The square matrix $M(\beta_0)$ depends upon β_0, the geometry of the structure, and the number of harmonics combined. Because arbitrary perturbations in B can be made from the correct fields and the result of 0 still remains on the left hand side of 25, the determinant of $M(\beta_0)$ must be 0. Bevensee's technique proceeds in two steps:

(1) Search for the β_0 which makes $\det[M(\beta_0)] = 0$

(2) Find the eigenvector corresponding to the zero eigenvalue and interpret this as the set of coefficients.

Bevensee justifies his formula as an application of an eigenvalue problem developed by Morse and H. Feshbach.[11] In this

derivation he has used trial fields which satisfy boundary conditions by means of smoothing functions within a transition region. As the transition region becomes smaller, the eigenvalue estimate of $\omega(\beta_0)$ becomes Bevensee's formula. This shows that the β_0 found by Bevensee's solution is such that $\omega(\beta_0)$ is an upper bound, which implies that β_0 is either an upper bound or lower bound depending upon the slope of the ω-β dispersion relation.

E. Reaction Method

The reaction method was developed by Rumsey in 1954.[10] Virtually all variational expressions can be derived directly by the application of the reaction concept. Harrington,[11] in particular, has developed variational formulas using the reaction method for cavities and wave guides.[12] Moreover, he has treated problems of inhomogeneously-filled wave guides with trial fields having discontinuities across a surface. These discontinuities are not as severe as those needed by Bevensee because his boundary value problem was with only one of $\vec{E}$ or $\vec{H}$ and along a surface with one coordinate constant. Nevertheless, the reaction method can easily incorporate the trial fields of Bevensee. In this section, the reaction integral is first presented. Bevensee's method is derived from the viewpoint of reaction. In later sections, the reaction formulation will be used in discussions of convergence of Bevensee's formula. Modification of the variational expression will be made based upon principles of the reaction method.

Denote the fields produced by sources $\underline{a}$ alone as $\vec{E}_a$, $\vec{H}_a$, and the fields produced by sources $\underline{b}$ alone as $\vec{E}_b$, $\vec{H}_b$. The reaction of fields $\underline{a}$ on sources $\underline{b}$ is defined as

$$\langle \underline{a}, \underline{b} \rangle = \iiint_V (\vec{E}_a \cdot \vec{J}_b - \vec{H}_a \cdot \vec{M}_b) dV \quad . \tag{26}$$

Reaction is closely linked to reciprocity, which in the above notation becomes

$$\langle \underline{a}, \underline{b} \rangle = \langle \underline{b}, \underline{a} \rangle \quad . \tag{27}$$

For waveguide problems, it is important to use an adjoint system to $\underline{a}$, denoted $\underline{a}^*$ consisting of fields E_a^*, $-H_a^*$ produced by sources M_a^*, $-J_a^*$. For homogenous regions, $\underline{a}^*$ corresponds to the field distribution traveling in the direction opposite $\underline{a}$ along the longitudinal direction of the wave guide.

When systems $\underline{a}$ and $\underline{b}$ have the same longitudinal propagation constant, the reaction of fields $\underline{a}^*$ on source $\underline{b}$ becomes a surface integral

$$\langle \underline{a}^*, \underline{b} \rangle = \iint_S \vec{E}_a^* \cdot \vec{J}_b + \vec{H}_a^* \cdot \vec{M}_b \, dS \quad , \tag{28}$$

and reciprocity is expressed by

$$\langle \underline{a}^*, \underline{b} \rangle = \langle \underline{b}, \underline{a}^* \rangle \quad , \tag{29}$$

$$\langle \underline{a}^*, \underline{b} \rangle = -\langle \underline{b}^*, \underline{a} \rangle^* \quad . \tag{30}$$

In variational analyses, reaction can be viewed as a measure of equivalency.[12] In fact, a source must have the same reaction with all fields equivalent over its extent so reaction is a necessary, though not sufficient, test for equivalent fields. For the source-free modes sought by our analysis of helical slow-wave devices, the correct fields, $\vec{E}_c$ and $\vec{H}_c$, are unsupported by currents away from the conducting walls. As a consequence, if an arbitrary system $\underline{a}^*$ has fields which satisfy the correct boundary conditions at conducting surfaces, the reaction of fields of $\underline{a}^*$ on the currents of the

exact system, which are only at the conducting walls, is zero:

$$\langle a^*, c \rangle = \langle c^*, a \rangle = 0 \quad . \tag{31}$$

Bevensee's formula can be recovered directly from Equation 31. Although the fields of system a satisfy the same boundary conditions as the correct system, fields of a may be supported by currents inside the wave guide. For Bevensee's trial fields, compensating currents are added to make the fields continuous at the free space trial region interfaces and to set the tangential electric field to zero at the tape. Specifically, we add currents

$$\vec{M}_n^T = -\hat{n} \times \vec{E}_n \tag{32}$$

to force the tangential field to zero on this conductor, where n is the harmonic number and T denotes tape. Simultaneously, currents

$$\vec{M}_n^o = -\hat{m} \times (\vec{E}_n^I - \vec{E}_n^{II}) \quad , \tag{33a}$$

and

$$\vec{J}_n^o = +\hat{m} \times (\vec{H}_n^I - \vec{H}_n^{II}) \tag{33b}$$

are added to remove the discontinuity in electric or magnetic fields at the other interfaces of trial functions regions (I) and (II). Because Bevensee's trial functions are source-free except at the interface of his trial function regions and because the trial functions satisfy Maxwell's equations, the surface integral of Equation 24 becomes a line interval at the interface of these regions. The properties of Bevensee's formula follow from postulating that the correct field is an exact sum of

trial fields. For the case of an external homogeneous dielectric support, for example, the longitudinal waves are the infinite sum

$$\begin{bmatrix} E_z \\ H_z \end{bmatrix} = e^{-j\beta_0 z} \sum A_n(r) e^{jn(\theta - \frac{2\pi}{p}z)} \quad , \tag{34}$$

where the radial portion is proportional to a modified Bessel function and depends upon region:

$$A_n(r) = \begin{cases} \begin{bmatrix} C_{1n} & I_n(\gamma_n r) \\ C_{2n} & I_n(\gamma_n r) \end{bmatrix} & r < r_{tape} \\ \begin{bmatrix} C_{3n} & R_n(\gamma_n r) \\ C_{4n} & S_n(\gamma_n r) \end{bmatrix} & r > r_{tape} \end{cases} \quad . \tag{35}$$

The series is truncated and the coefficients are collected into one column vector denoted C. Equation 31 indicates that the reaction of the correct system with an approximate system is always zero. If the approximate system $\underline{a}$ is taken as a second collection of trial fields using coefficients B, the reaction integral becomes the quadratic form

$$B^{\dagger} M(\beta_0) C = 0 \tag{36}$$

for any arbitrary coefficients in B. This implies that the $\det[M(\beta_0)]$ is zero for the correct system of fields. Notice that unlike Bevensee's argument a perturbation did not have to be invoked in concluding that the determinent of $M(\beta_0)$ is zero. Bevensee needs a perturbation because he starts with the self reaction $\langle \underline{c}^*, \underline{c} \rangle$. Our technique uses the reaction on the

field of a second system directly. In fact, in our formulation, arbitrary perturbations of coefficients in B are just another set of coefficients.

F. Variational Nature of the Reaction Integral

If the system $\underline{b}$ or $\underline{a}$ is not an exact sum of trial fields, suppose we include a perturbation $\underline{p}$ in the systems $\underline{a}$ and $\underline{b}$ from the correct system: $\underline{b}^* = C^* + \varepsilon \underline{p}_b^*$, $\underline{a} = C + \lambda \underline{p}_a$ where ε and λ are small numbers. The reaction $\langle b^*, a \rangle$ is then variational about 0. That is,

$$\langle b^*, a \rangle = \varepsilon\lambda \langle p^*, p \rangle \quad , \tag{37}$$

which is variational in the sense that

$$\left. \frac{\partial \langle b^* a \rangle}{\partial \varepsilon} \right|_{\substack{\lambda=0 \\ \varepsilon=0}} = 0 \tag{38}$$

and

$$\left. \frac{\partial \langle b^* a \rangle}{\partial \lambda} \right|_{\substack{\lambda=0 \\ \varepsilon=0}} = 0 \quad . \tag{39}$$

For Bevensee's solution to succeed, one does <u>not</u> depend upon this variational property. Instead, ε must be a small number. Specifically, after truncation to N harmonic trial fields, one assumes that the difference of the field with the best selection of coefficients from the true fields is such that

$$\langle \underline{a}^*, \underline{b} \rangle = \varepsilon \langle \underline{a}^*, \underline{p}_b \rangle \tag{40}$$

is very small. This concept will be discussed in greater detail when convergence of Bevensee's method is discussed in Section VII.

G. Symmetric Properties from Reaction

Bevensee's formula has been shown to be a quadratic form given by Equation 25. Also, it was derived as a reaction integral. Symmetric properties of the variational matrix follow from reciprocity expressed as reaction integrals. In particular, Equation 30 becomes the matrix equation

$$B^{\dagger}MC = -(C^{\dagger}MB)^* \quad . \tag{41}$$

One concludes

$$M = -M^{\dagger} \quad . \tag{42}$$

Also, the matrix M can be made purely imaginary by scaling all TM field coefficients by $e^{+j\pi/4}$ and all TE coefficients by $e^{-j\pi/4}$. Because $M(\beta_0)$ is a pure imaginary symmetric matrix, all TE waves are in phase as are all TM fields. The TE and TM modes are out of phase by π radians. In addition, symmetry allows the matrix to be filled using only the upper triangular elements. This is particulary useful when numerical integrations are needed in the computation of elements.

SECTION IV

COMPUTATIONAL RESULTS FOR THE VARIATIONAL ANALYSIS OF A SHEATH HELIX

Current spiralling along an infinite cylinder in free space is known as a sheath helix. It is a configuration for which the analytic solution of the field distributions are explicitly known.[1] The correct fields are linear combinations of those trial fields written earlier in Equations 5(III) through 10(III).

In applying the variational technique to this problem, the propagation constant and trial field coefficients were initially unknown. Each trial function harmonic, n, can form an independent sheath mode. The variational matrix had dimension 4 x 4. By finding the β_0 corresponding to a singular matrix, the correct dispersion relation was found. Figure 7 shows that the exact dispersion can be recovered for the n=0 mode. The exact relative magnitude of the coefficients also was found as the eigenvector corresponding to the zero eigenvalue. We were also able to recover correct solutions for higher harmonics.

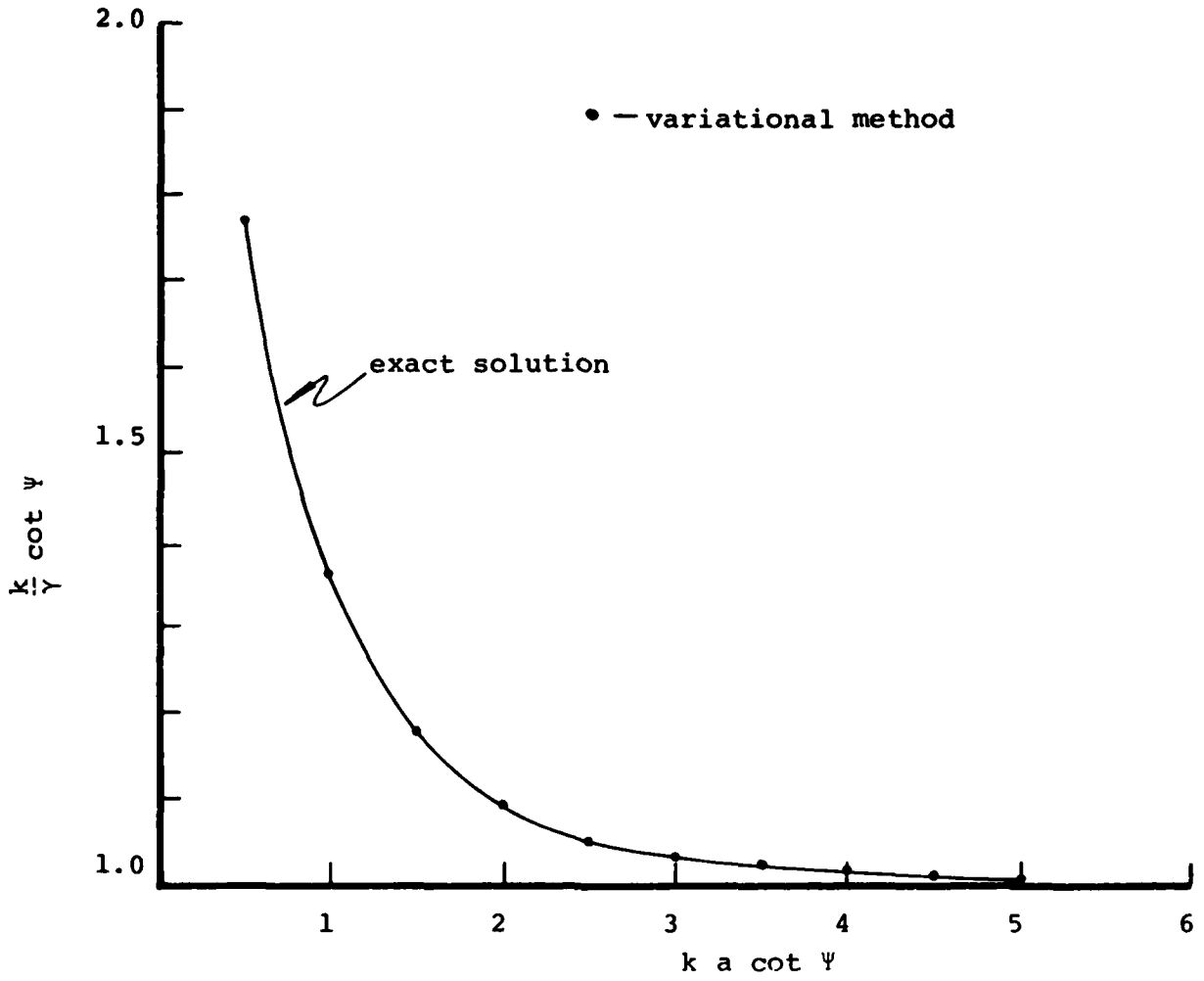

Figure 7. Comparison between the exact dispersion solution for the sheath helix and that found by the variational method.

SECTION V

VARIATIONAL ANALYSIS OF A HELICAL TAPE SUPPORTED BY AN HOMOGENEOUS DIELECTRIC REGION

This case differs from the sheath-helix analysis in that the current is confined to a helically wrapped tape. Unlike the sheath harmonics, the internal and external trial fields are continuous over part of their interface as shown in Figure 4a.

At first four independent trial fields per angular harmonic were combined in the variational technique. Unlike the sheath case, the angular harmonics do not decouple. Computational results were compared to those from a program based upon Paik's analysis[5] because it assumes an homogeneous external dielectric. As will be shown, results for some combinations of harmonics were excellent. However, spurious solutions appear with bad impedances. Two techniques were developed to remove spurious solutions. One made a modification to the variational expression. A second method added continuity constraints which reduced the number of independent trial field coefficients. Both approaches are presented in this section.

A. Four Coefficients Per Angular Harmonic

When the variational technique was applied to the homogeneous support structure, two trial field regions were used. A TE and TM mode for each harmonic were placed in the trial region inside the tape radius and in the region covering the dielectric. Consequently, four trial fields are used for each angular harmonic. For N harmonics combined in the analysis there are 4N unknown coefficients and the variational matrix has dimension 4N x 4N.

First, problems with an external free space region were examined. The geometric configurations of the structures examined are the same as those found in the Northrop final report on the metal ceramic helix,[11] except that a dielectric or vacuum is placed in the external region. The pertinent dimensions are found in Appendix A. Helix No. 2 was selected because the approximations made in the Paik analysis are best for a small gap-to-pitch ratio.

For the case of a single trial-field harmonic, (n=0), no solution to the dispersion relation was found. For the case of three harmonics (0,-1,1), two solutions close to the expected dispersion value from the Paik theory were found. The higher β_0 of these two yielded the best impedance. Results for this β_0 from 10 to 20 GHz are compared to Paik in Figures 8 and 9. The agreement in impedance is excellent. The values of phase velocity using Paik are higher than those from the variational analysis, but they are parallel.

As the number of trial field harmonics is increased, the solution does not necessarily improve. When three harmonics were combined, an examination of the field values at the interface of the trial regions showed the electric field to be in phase across the interface, while the magnetic field was π radians out of phase. This is a proper configuration on the conducting tape, but an incorrect state for the free-space portion of the interface. As the number of trial fields increased, the magnetic field remained discontinuous along the free-space portion of the interface.

The impedance and dispersion for Helix No. 4 at 6 GHz for various combinations of trial fields are shown in Table 1. Note that multiple solutions again can be found. The results do not appear to converge. As will be shown, the variational

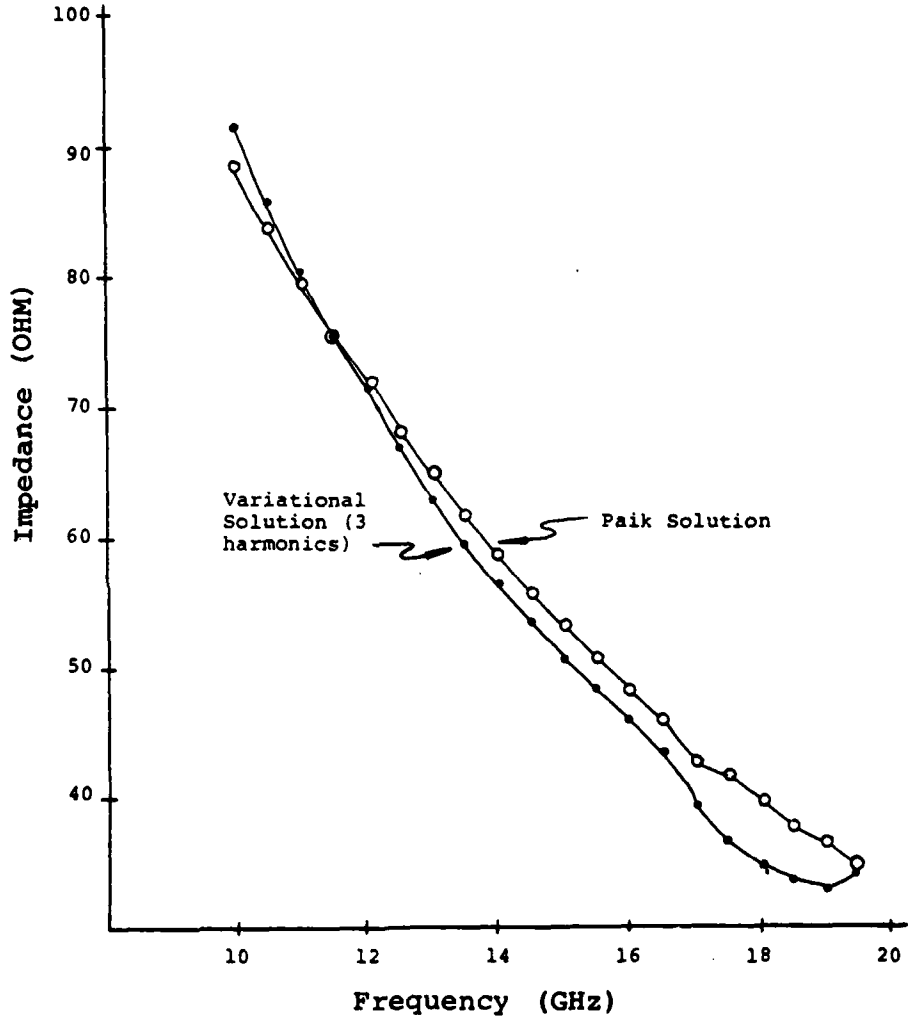

Figure 8. Comparison between impedance at the tape from Paik theory and variational method for Helix No. 2 without dielectric.

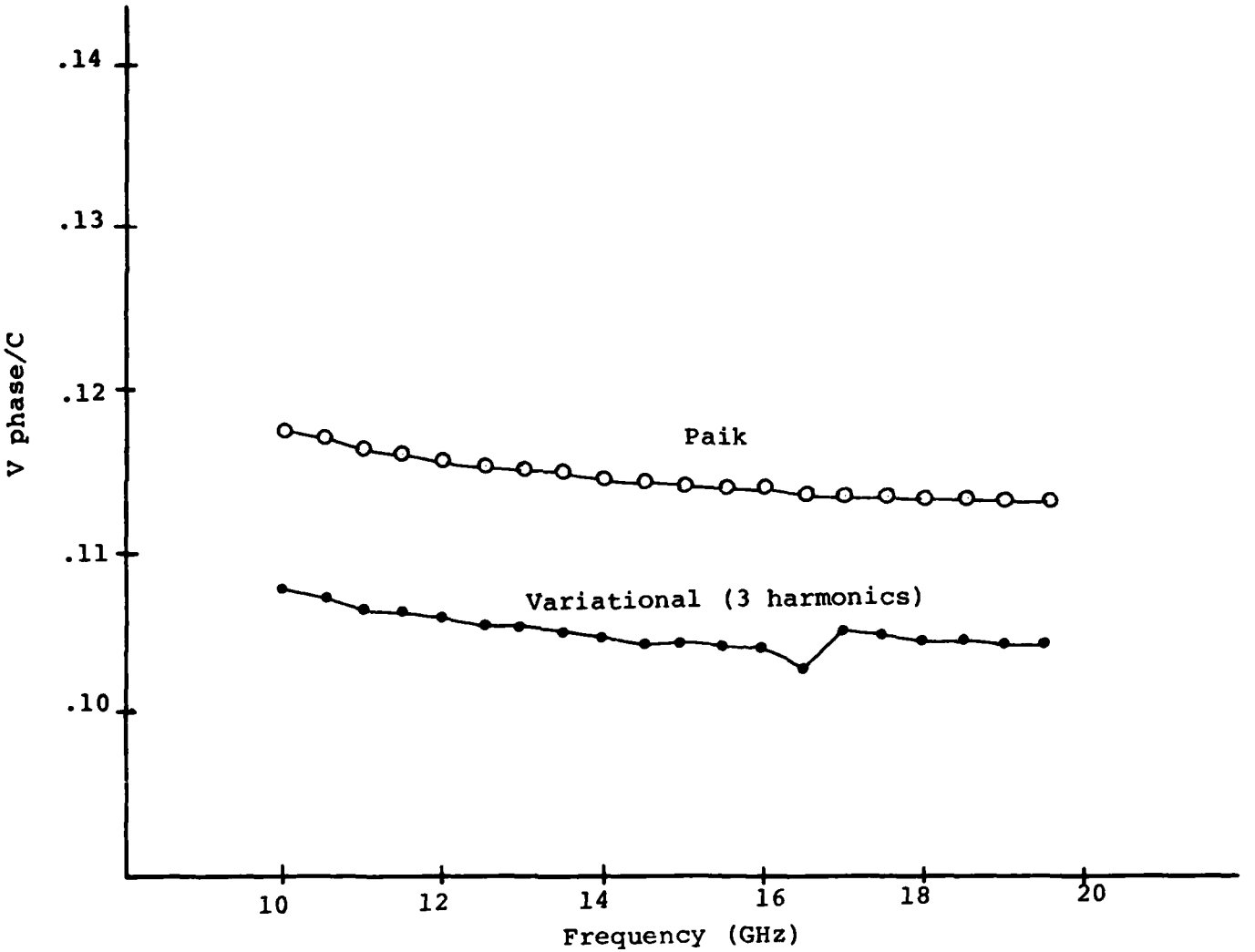

Figure 9. Comparison between phase velocities from Paik theory and variational method for composite Helix No. 2 without dielectric.

TABLE 1

PHASE VELOCITY AND IMPEDANCE FOR HELIX NO. 4

WITHOUT DIELECTRIC AT 6 GHz USING FOUR TRIAL FIELDS PER HARMONIC

Number of Trial Field Harmonics	Phase Velocity/ Speed of Light	Impedance at Tape
3	.239	.46
3	.192	2.24
5	.258	39.7
7	.202	44.1
9	.228	81.3
9	.233	72.6
11	.438	72
13	.259	38
19	.231	123.1
Paik	.245	88.3

technique had to be modified before convergent results with correct values could be obtained.

B. Spurious Propagation Constants

In variational analysis, the measure of an equivalent field is an identical reaction on the currents. Uniqueness is not guaranteed and, therefore, multiple solutions are possible.

The existence of multiple propagation constants makes the automatic choice of the best solution difficult. In searching for the best solution one is forced to consider the degree to which specific proper boundary conditions have been met.

Multiple solutions do not disappear as more harmonics are added to the trial fields. It is also possible to have but one solution with a particular combination of trial field modes and none with another.

In an attempt to remove difficulties associated with multiple solutions, we have used constraints or added additional variational terms. These methods are described in the following sections. The conventions used in the remainder of this report is that the lowest β_0 is the best solution. Convergence of impedance and phase velocity are examined with this convention. In theory, if all spurious solutions could be removed, the higher harmonics of the slow wave structure could also be predicted.

C. Use of Reaction Method to Generate a New Convergent Variational Expression

The reaction method provides a means for devising additional variational expressions by manipulating trial-field currents.

As noted previously, the electric and magnetic currents are added to the system so that the boundary conditions of the correct fields are met. These are

$$\vec{J}_n = \hat{m} \times (\vec{H}_I - \vec{H}_{II}) \quad (1)$$

and

$$\vec{M}_n = -\hat{m} \times (\vec{E}_I - \vec{E}_{II}) \quad , \quad (2)$$

where n refers to the trial field harmonic and $\hat{m}$ is a normal at the interface of trial region I and II. Figure 10 depicts adding a current on one side of the interface and cancelling it on the other so that the boundary conditions are undisturbed. Taking the currents as $\vec{J}_n$ and $\vec{M}_n$, an additional term arises in the variational expression. This is a method for weighing some currents more than others.

Convergence of impedance and phase velocity have been examined, using the revised formula. The lowest β_0 was taken as the solution. The spurious β_0's were removed. Figures 11 through 13 show the improvement we found at 10 GHz in the convergence of the electric field as the number of modes in the trial fields are increased. Tangential H-field at the interface of trial field regions remains 180° out of phase. Table 2 shows convergence of the impedance as the number of modes increases.

D. Continuity Constraints at the Trial Field Interface

Because the tape is radially thin, both the correct outer and inner tangential electric fields are zero at the same interface of the trial field regions. Since continuity already exists on the free-space interface, this continuity exists for all angles at the interface surface.

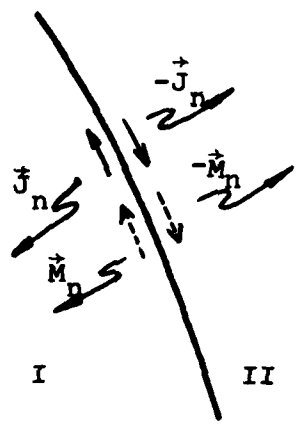

Figure 10. Cancelling additional currents across the interface of trial field regions.

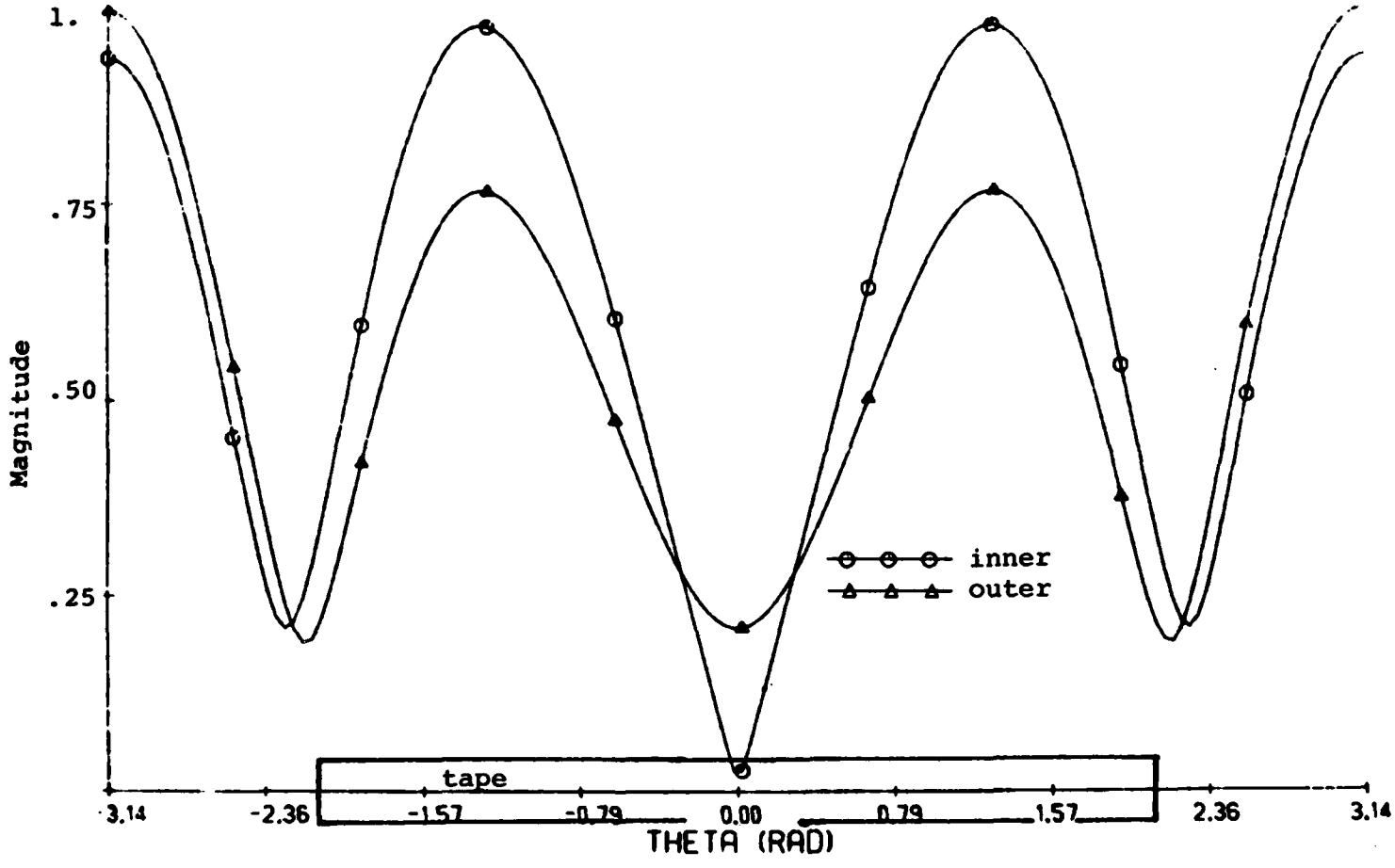

Figure 11. Tangential E boundary values at tape radius using five harmonics.

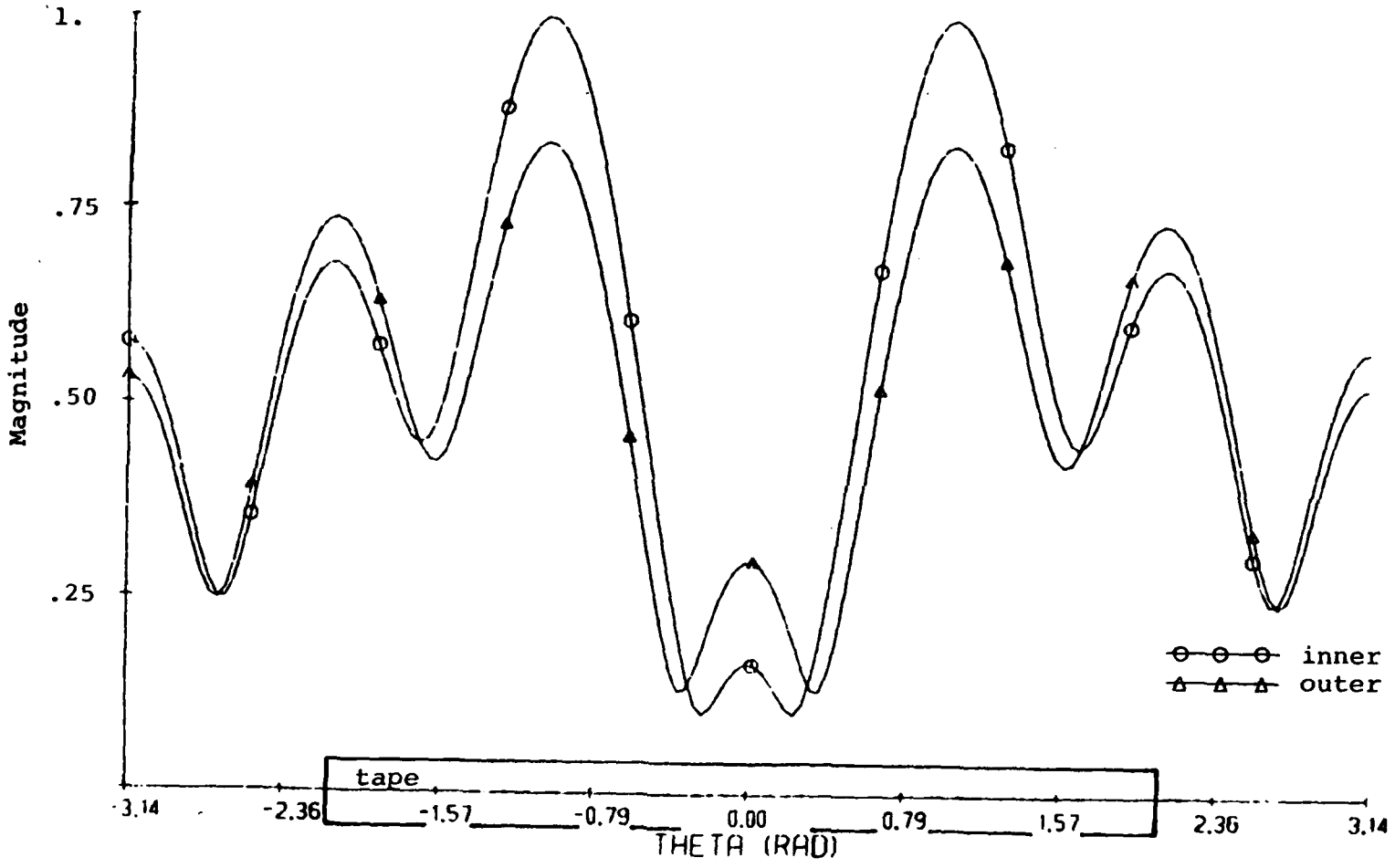

Figure 12. Tangential E boundary values at tape radius using seven harmonics.

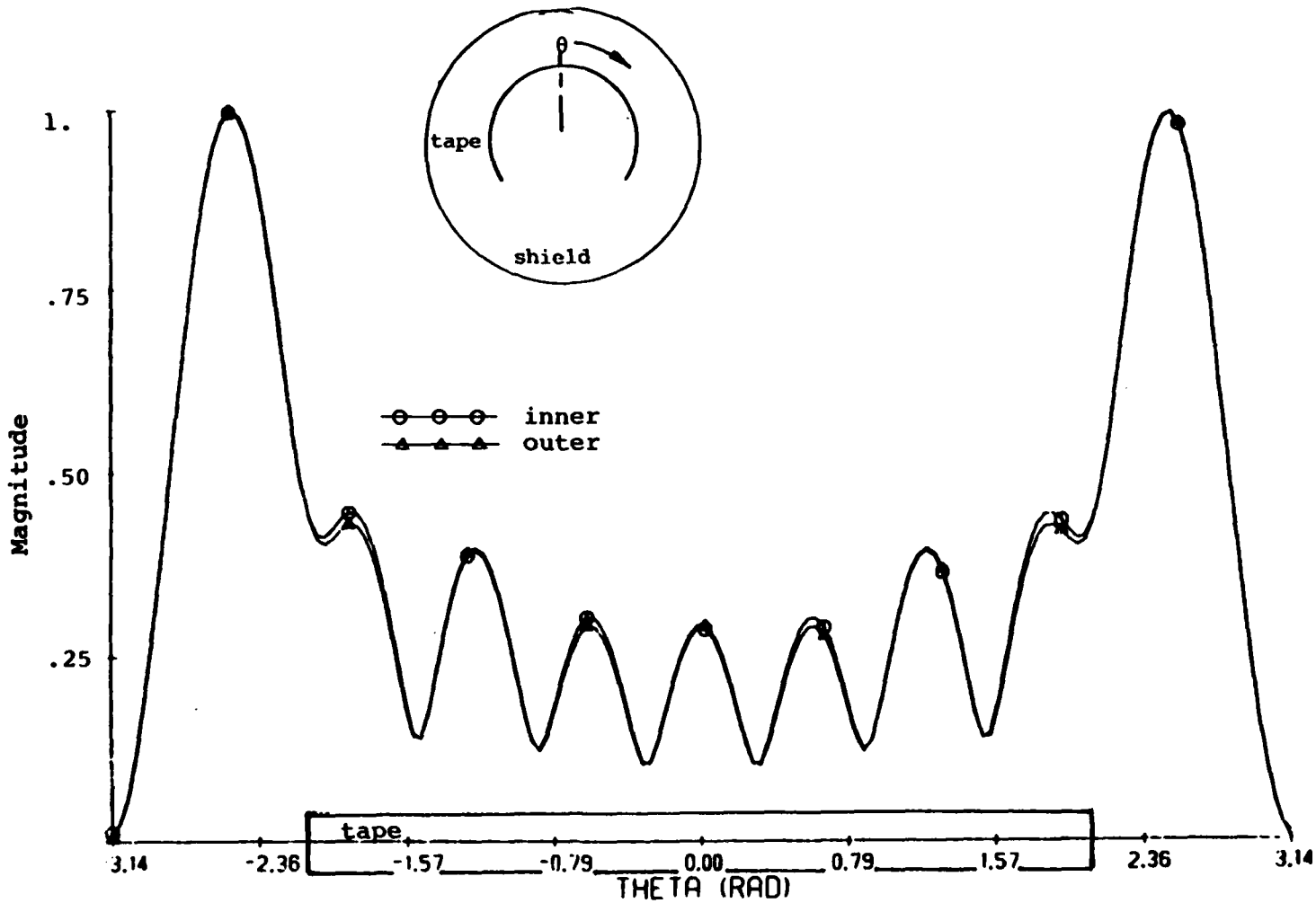

Figure 13. Tangential E boundary values at tape radius using 11 harmonics.

TABLE 2

TRENDS USING NEW VARIATIONAL EXPRESSION ON COMPOSITE HELIX NO. 2 WITHOUT DIELECTRIC

New Variational Expression at 10 GHz:

No. Harmonics	$V_p/C \times 10^{+1}$	$Z_1(\Omega)$
5	1.09	183
7	1.13	172
11	1.13	77
13	1.12	97.1

Paik Theory:

7	1.17	88.4

V_p - phase velocity

C - speed of light

The angular dependence of the trial fields is contained in the phase by Equation 2. It can be concluded that the continuity constraint in tangential electric field should be satisfied by each harmonic, n, of the trial fields because the exponentials, $e^{jn\theta}$ are orthoginal over 2π. A careful examination of the spurious solutions shows that this constraint is not satisfied for each n. Consequently, some false β_0's can be removed by explicitly enforcing this constraint.

Simultaneously, the number of independent field coefficients per trial field harmonic is reduced from four to two. Numerically, this has the advantage of reducing the size of the variational matrix from 4N x 4N to 2N x 2N, where N is the total number of trial field harmonics. Moreover, because tangential electric fields are constrained to be equal, the extra variational terms added in the last section by the modified variational expression vanish. The problem is simpler because only two types of mismatch in the boundary condition remain: (1) the deviation from 0 of the tangential electric field at the tape, and (2) a noncontinuous magnetic field at the free-space interface.

E. Use of Constraints to Obtain Convergent Results for Impedance and Dispersion

By constraining the tangential electric field, the fields and dispersion converge as the number of trial-field harmonics increases. In addition, the true propagation constant is close to the lowest solution of $[\det M(\beta_0)] = 0$. For Helix No. 2, with or without dielectric in the external region, results are particularly close to those produced from the Paik theory. Tables 3, 4, 5 and 6 show the behavior of impedance and dispersion as the number of harmonics increases. In Figures 14 through 17

TABLE 3

HELIX NO. 2 WITHOUT DIELECTRIC GAP/PITCH = .35

No. of Harmonics		10 GHz		15 GHz		20 GHz	
		$V/_PC$	Z (Ω)	V_P/C	Z_1 (Ω)	V_P/C	Z_1 (Ω)
3		.108	93.6	.105	37.8	.104	20.0
11		.112	73.7	.107	35.7	***	***
17		.112	84.7	.109	47.2	.108	33.1
23		.113	88.9	.105	53.6	.110	33.3
Paik (7 modes)	1	.117	88.4	.115	53.2	.113	32.9
ka		.23		.34		.46	

V_P - phase velocity of 0-order harmonic
Z - impedance of 0-order harmonic
C - speed of light
*** - no singular matrix found
a - tape radius

TABLE 4

HELIX NO. 2 WITH DIELECTRIC GAP/PITCH = .35

No. of Harmonics	10 GHz V_p/C	10 GHz Z (Ω)	15 GHz V_p/C	15 GHz Z_1 (Ω)	20 GHz V_p/C	20 GHz Z_1 (Ω)
Variational						
3	.0605	28	***	***	***	***
17	.0618	32	.0619	23.45	.0619	17.62
23	.0623	36	.0625	27.5	.0626	20.62
Paik (7 modes)	.0639	40.3	.0641	29.8	.0645	18.9
Measured by Northrop	.085		.09	9.5	.092	5.1

V_p - phase velocity of 0-order harmonic

Z - impedance of 0-order harmonic

C - speed of light

*** - no singular matrix found

NOTE: Both the variational analysis and Paik theory used an homogenous dielectric which was the average dielectric by volume in Northrop's spiral dielectric structure. ($\epsilon_D = 4.72$)

TABLE 5

HELIX NO. 1 WITHOUT DIELECTRIC GAP/PITCH = .49

No. of Harmonics	2 GHz		5 GHz		8 GHz	
	V_p/C	Z(Ω)	V_p/C	Z(Ω)	V_p/C	Z(Ω)
17	.1671	113.5	.151	87.4	.147	63.1
23	.167	22.9	.153	9.5	.148	3.2
29	.167	113.1	.153	89.8	.149	59.0
37	not done		.154	84.8	not done	
Paik (7 modes)	.1632	114.7	.1554	75.3	.1523	42.23
ka	.110		.276		.442	

V_p - phase velocity of 0-order harmonic

Z - impedance of 0-order harmonic

C - speed of light

a - tape radius

TABLE 6

HELIX NO. 4 WITHOUT DIELECTRIC GAP/PITCH = .77

No. of Harmonics	2 GHz		5 GHz		8 GHz	
	V_p/C	Z(Ω)	V_p/C	Z(Ω)	V_p/C	Z(Ω)
17	.250	68.7	.270	70.4	.255	60.0
2	.253	69.7	.250	66.3	.257	64.1
Paik (7 modes)	.236	100.9	.245	91.4	.245	82.3
ka	.062		.155		.245	

V_p - phase velocity of 0-order harmonic
Z - impedance of 0-order harmonic
C - speed of light
a - tape radius

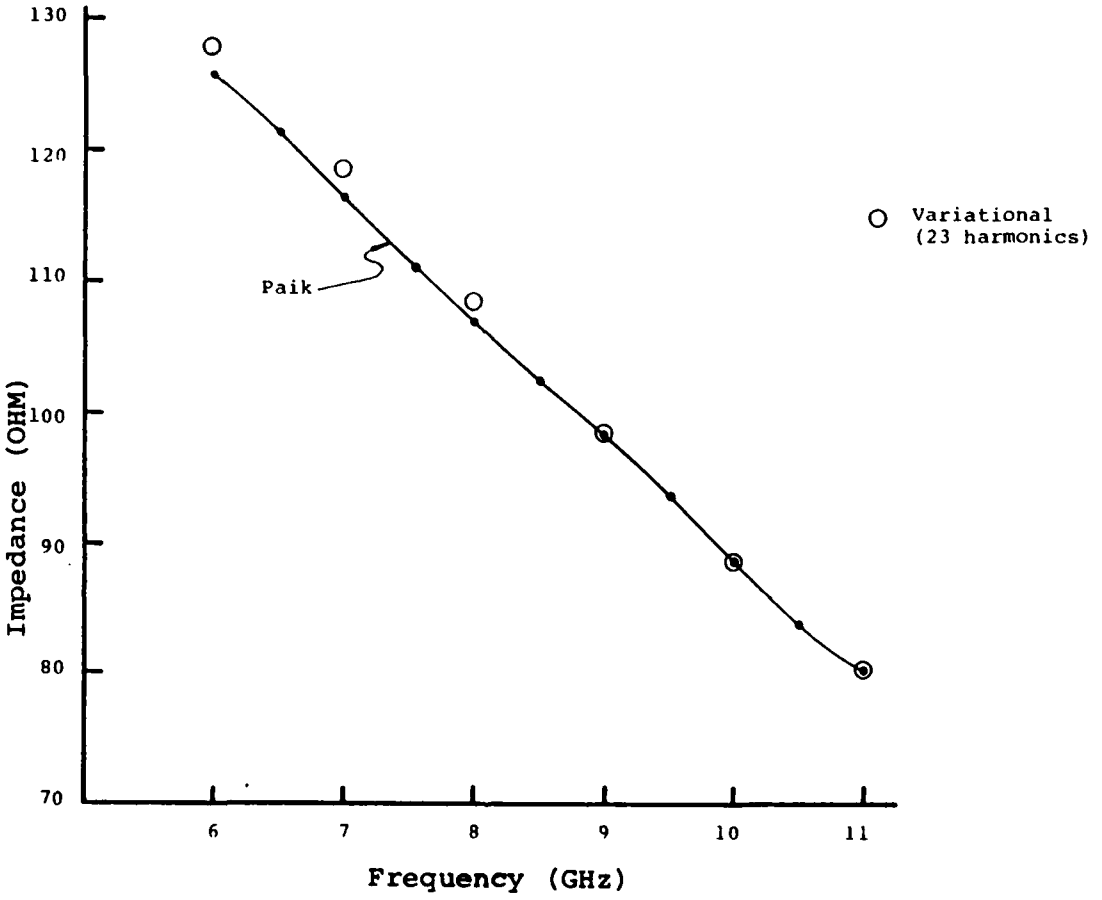

Figure 14. Comparison using 23 harmonics between impedances at the tape from variational method and Paik theory applied to Helix No. 2 without dielectric.

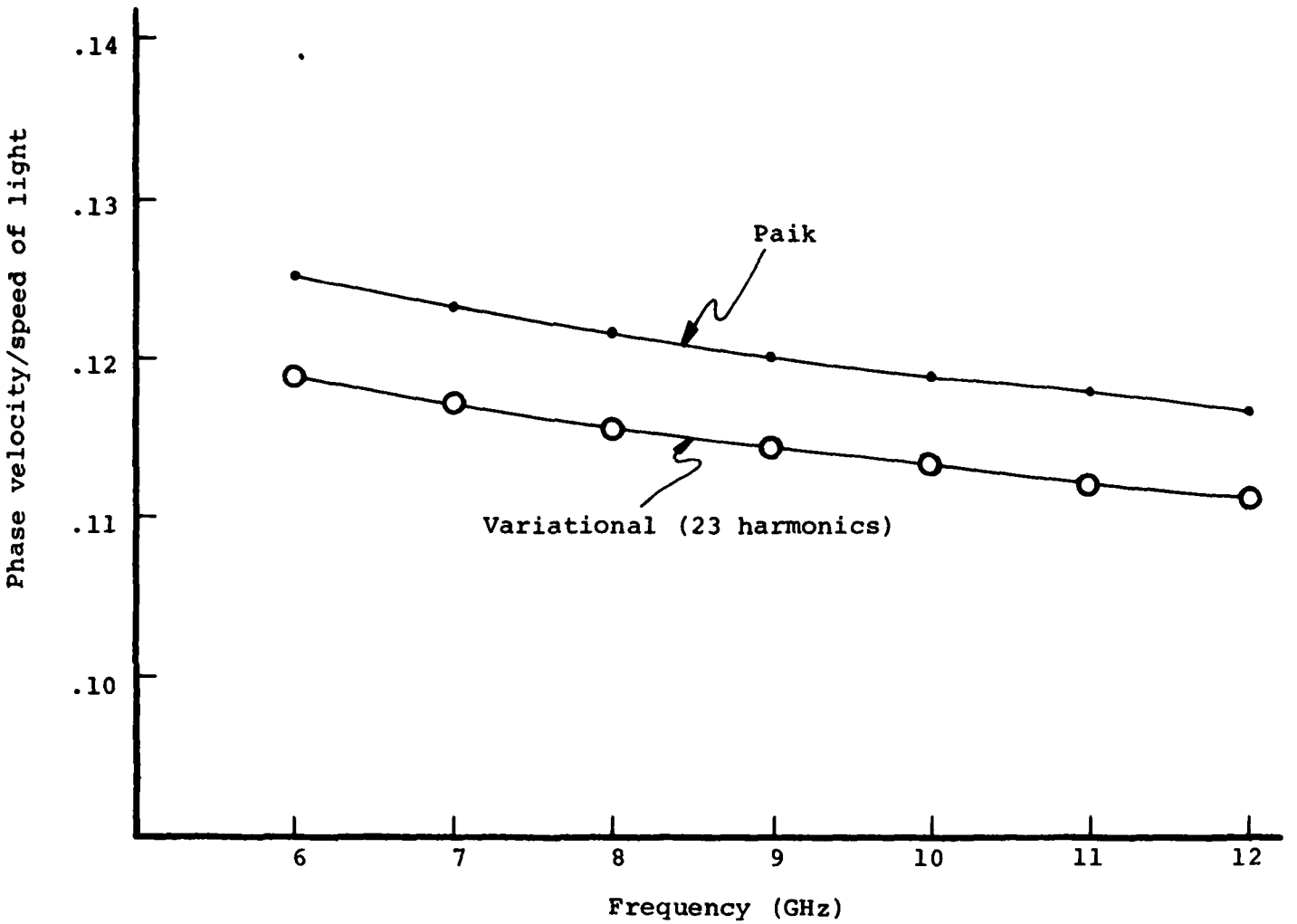

Figure 15. Comparison using 23 harmonics between phase velocities from variational method and Paik theory applied to Helix No. 2 without dielectric.

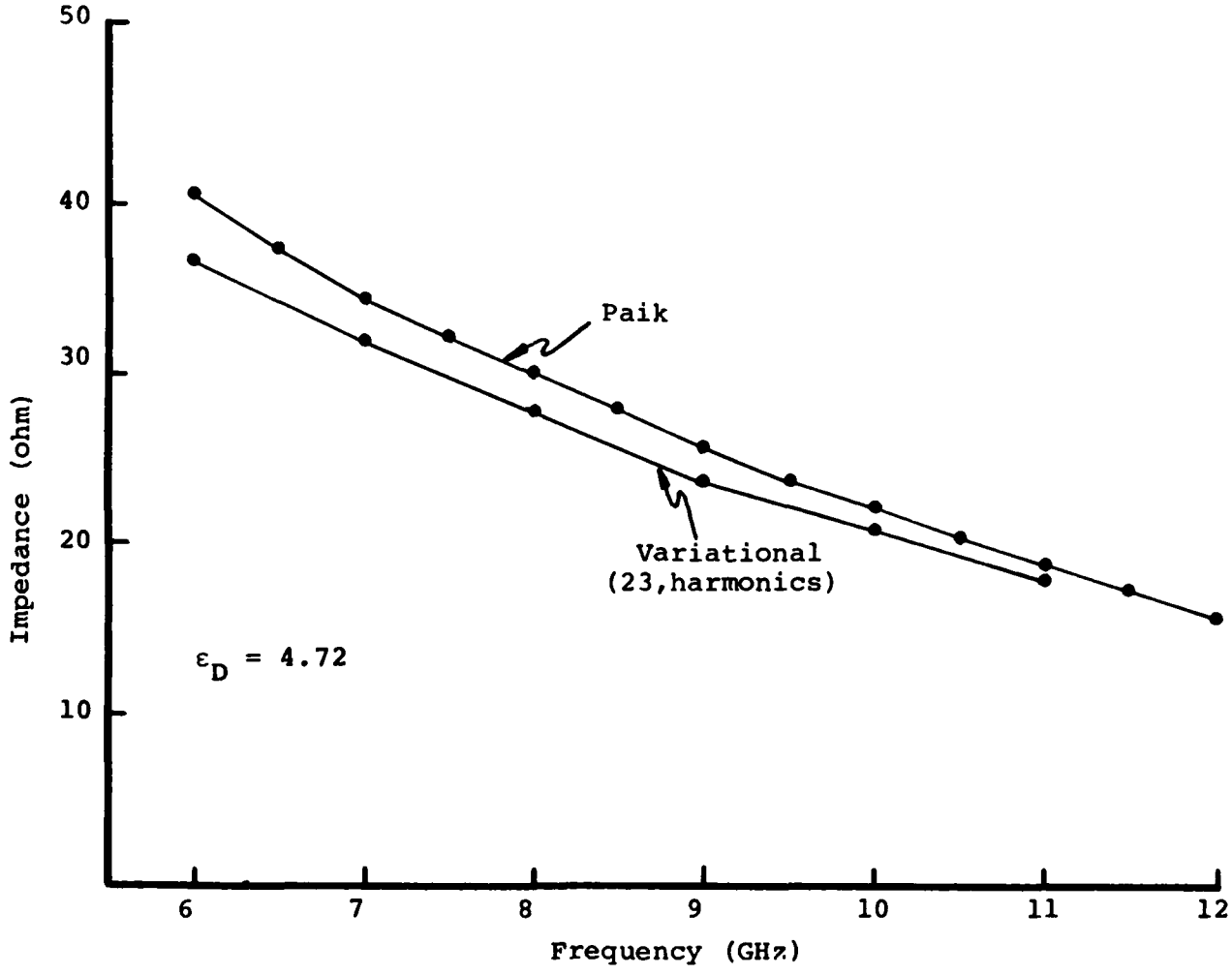

Figure 16. Comparison using 23 harmonics between impedance at the tape from variational method and Paik theory applied to Helix No. 2 with mean dielectric.

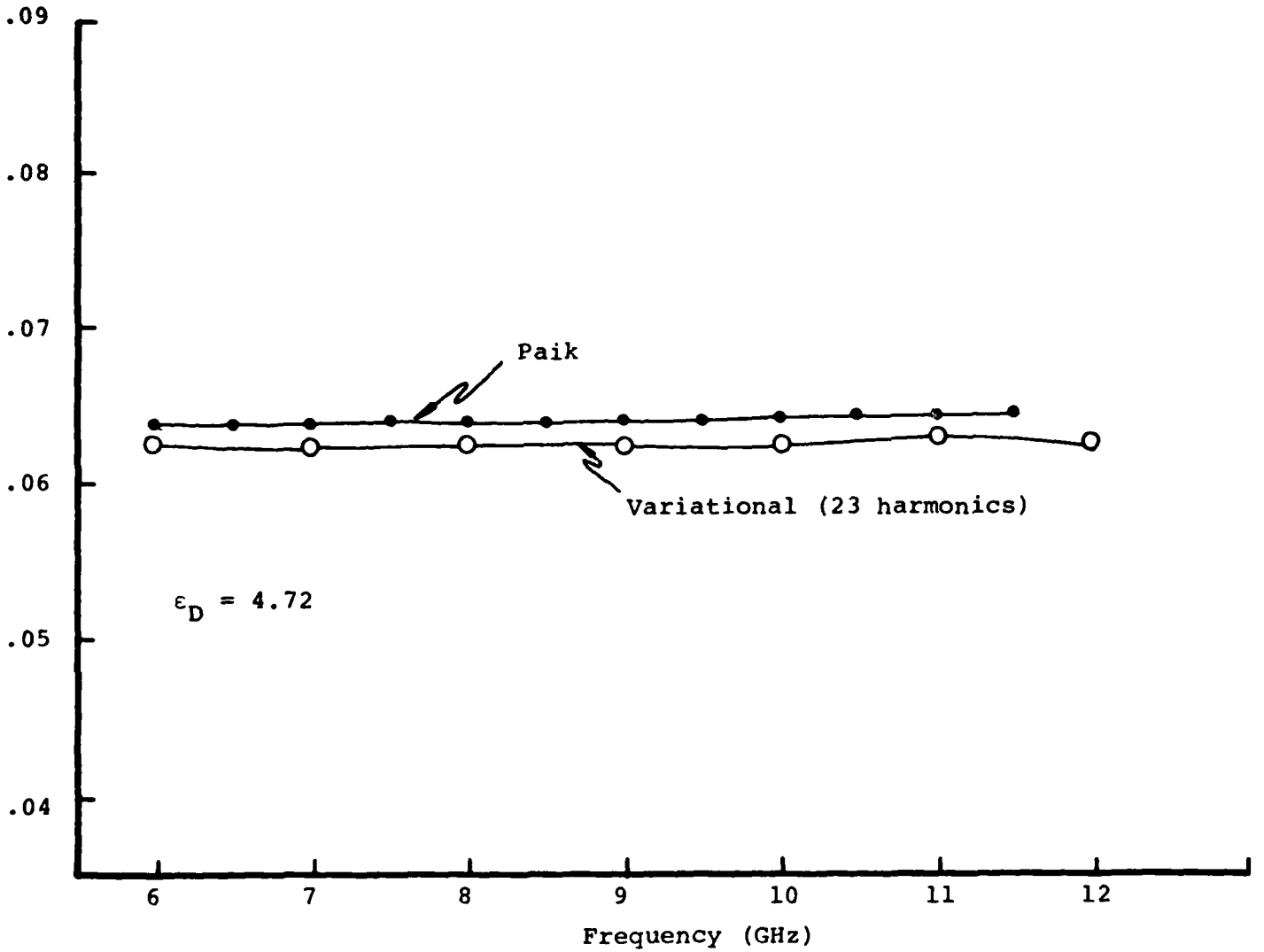

Figure 17. Comparison using 23 harmonics between phase velocities from variational method and Paik theory applied to Helix No. 2 with mean dielectric.

a comparison between the Paik theory and the variational analysis is made over an octave in frequency using Helix No. 2. Results with and without an external dielectric are shown using 23 trial field harmonics. Excellent agreement in both impedance and dispersion is found. Table 3 shows there is improvement in the impedance and phase velocity as the number of harmonics increases. In Table 4 some results at three frequencies for Helix No. 2 with a homogeneous dielectric are shown. At the few combinations examined, results improve as more modes are combined. In Table 5, results for Helix No. 1 without dielectric at three frequencies are given. Phase velocity is again similar to that calculated from Paik's theory. Impedance is in good agreement with Paik's at the lowest frequency, but it differs increasingly more at the higher frequencies. The Paik analysis used assumed a constant field in the gap region. As the gap to pitch ratio increases, this approximation should yield poorer impedances. In Table 5 some results for a large gap to pitch ratio are presented. By increasing the number of harmonics from 17 to 27, impedance and phase velocity do not change greatly. Impedances differ greatly from Paik's.

Although the impedance and phase velocity are better behaved, an examination of the boundary fields indicates that the magnetic field has remained π radians out of phase across the free-space interface even when large number of harmonics are combined. In some cases there appears to be a larger current at the free-space interface than on the metal tape. The current on the tape usually peaks at the ends of the tape as it should.

Lack of continuity of the H-field free-sapce regions is attributed to Bevensee's choice of trial fields. In

Section VII and VIII, the need for additional trial fields is shown in detail. Bevensee avoided using these partly because they did not satisfy Maxwell's equation and thereby introduced volume integrals. In spite of Bevensee's set of trial fields, our results show that good convergent results can be attained if one uses a large number of harmonics.

The computer program, denoted HELIX, using two independent trial fields per angular harmonic, typically occupies about 90K of fast memory. Values of impedance, phase velocity, field coefficients and attenuation are calculated over a specified frequency range. CPU time grows exponentially with the number of trial field harmonics. Whereas a case at a single frequency using three harmonics typically consumes 4 seconds of CPU time, the same case analyzed with 23 modes may take some 90 seconds.

SECTION VI

VARIATIONAL ANALYSIS OF A SPIRAL DIELECTRIC SUPPORT

The metal-ceramic helix has a spiralling dielectric support (Figure 4), fabricated by depositing the ceramic on top of the helical tape. The great advantage of the variational method is that the geometry of their dielectric region is included in the variational expressions. The analyses of the spiral dielectric, slow-wave structures involve two types of models: (1) models with two trial field regions, and (2) models with three trial field regions.

A. Two Trial Field Regions

When two trial field regions are used, there are four trial fields per harmonic just as there were for the homogeneous support. However, the spiral dielectric introduces a new radial discontinuity in the external dielectric, in that the dielectric constant abruptly changes across the radial interface between free-space and ceramic (Figure 6).

The geometry of the support enters the variational formula as a volume integral. Specifically for a set of trial functions using dielectric constant ε_p, the first term of the variational formula in Equation 25(III) becomes

$$I_{vol} = \int_{\text{SPIRAL DIELECTRIC}} + j\omega(\varepsilon_p - \varepsilon_D)\, \vec{E}_+ \cdot \vec{E}_-^{*}\, dV_D$$

$$+ \int_{\text{SPRIAL FREE SPACE}} + j\omega(\varepsilon_p - \varepsilon_0)\vec{E}_+ \cdot \vec{E}_-^{*}\, dV_F \quad , \qquad (3)$$

where ε_p is the trial fields' dielectric and ε_D is that of the ceramic. Because the trial fields have a simple exponential dependence upon coordinates and 0, this volume integral reduces to an integration along the radius of the external region which must be computed numerically.

First, continuity constraints were applied at the tape radius so that only two independent coefficients per space harmonic exist. There were $\frac{N}{2}\left[1 + N\right]$ numerical integrations needed in the analysis, where N is the total number of trial field harmonics. Because the modified Bessel functions are asymptotically exponential and the correct fields should decay in the external region, the computational time was decreased by using an eight-point Gaussian quadrature integration scheme. Test cases with harmonic n=5, showed agreement between the Gaussian integration and more costly adaptive integration schemes through the fifth decimal place. By limiting the sampling of the integrand to eight fixed points, Gaussian integration schemes had the additional advantage of allowing components of the field at the sampled radii to be computed only once and stored. They were combined into several integrands when needed. This drastically reduced computational time in the numerical integrations.

The two independent coefficients per trial field harmonic analyses of the spiral dielectric were extremely sensitive to the dielectric of the external field region, ε_p. The use of a mean dielectric by volume yielded the best results. However, small changes resulted in large changes in the computed propagation constants. Numerical results were compared to experimental results listed in the Northrop final technical report on the composite metal-ceramic helix.[11] The simulated phase velocity for Helix No. 2 at 6 GHz was eighty percent of the measurement.

To give more freedom to the external trial fields, the continuity constraint at the tape was removed. This quadrupled both the size of the variational matrix as well as the number of numerical integrations required. This analysis was also extremely sensitive to the value of the dielectric used for the external trial field region. Best results were obtained for Helix No. 2 using an average dielectric for the external trial field region. Phase velocity was within about 15 percent of measured values for frequencies of 6 and 10 GHz. Results for Helix No. 4, which had a large gap-to-pitch ratio,were not nearly as good.

B. Three Region Problems

Because the two region analysis of the metal-ceramic helix was so sensitive to the trial-field dielectric, a three-region model was developed in which an additional set of TE and TM trial fields using the dielectric of the ceramic were placed over the spiraling-dielectric support. This meant that a total of six fields with harmonic dependence $e^{jn\psi}$ must be combined. The variational matrix takes on a size of 6N x 6N. Because the radial tape thickness can be as much as 50 percent of the tape-to-shield distance, the effective volume occupied by the dielectric was changed by the thin tape assumption. Therefore, a radially thick tape was modeled as shown in Figure 6. This required additional numerical integrations over the radial sides of the tape, where the tangential electric field was not zero. In this model, then, geometry is modelled exactly. No average dielectrics nor dimensions are assumed.

The three-region problem requires numerical integration in the computation of variational terms at the radial interface of the external, free-space region and dielectric region. As in

the two-region problem, these are integrations along the radius. Applying the symmetry of the reaction integral from Equation 37(III), the number of numerical integrations can be reduced from 16 per harmonic to 4. Counting the numerical integration along the sides of the tape, a total of $8 \cdot \frac{N}{2} \left[1 + N\right]$ numerical integrations are needed in combining all fields within N trial field harmonics. An eight point Gaussian-quadratic scheme was employed so that the field components could be computed and stored at fixed samples along the radius and combined into one of the many integrands when required. CPU time for this analysis is still considerable. Figure 18 shows the CPU time needed to make all calculations as a function of the number of trial fields combined when executed on the Harris 550. The time increases exponentially with the number of trial field harmonics.

At a frequency of 10 GHz on Northrop's ceramic Helix No. 2, convergence of dispersion and line impedance was examined as a function of the number of trial field harmonics. These results are shown in Figures 19 and 20. The harmonics combined were different for the runs summarized by Figure 20 in that certain harmonics, thought to cause numerical instability because they had little contribution to the total field, were excluded. The phase velocity is much more erratic than it had been for the homogenous support model. Impedance at the line varies even more, although deleting certain harmonics makes the values considerably more stable. Numerical comparisons between adaptive and eight-point Gauss-Quadrature integration indicates that for a large number of trial field harmonics, the precision of the Gaussian method in the power flow integration is down to two or three decimal places. This accounts for the divergence of impedance. It appears that more samples along the radius are needed in the numerical integration for better results at large combinations of harmonics for both impedance and

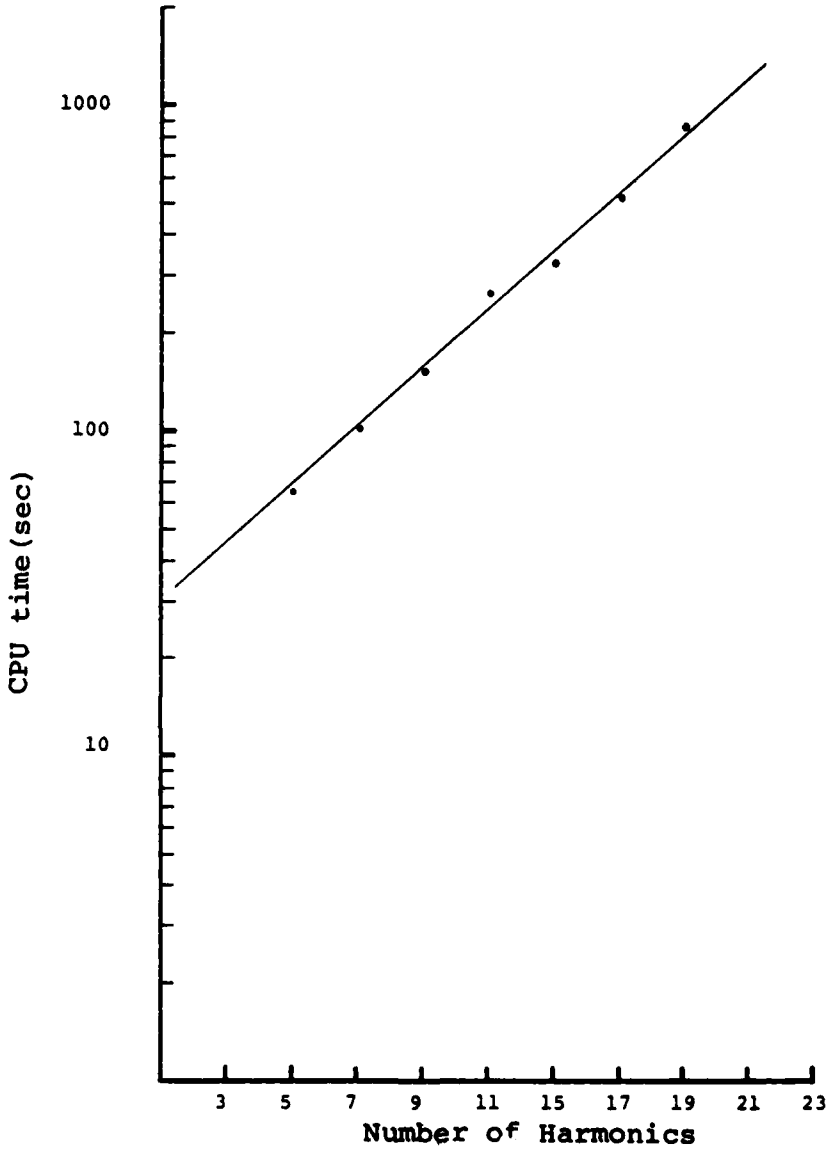

Figure 18. CPU time in three trial region spiral dielectric variational analysis as the number of harmonics increases.

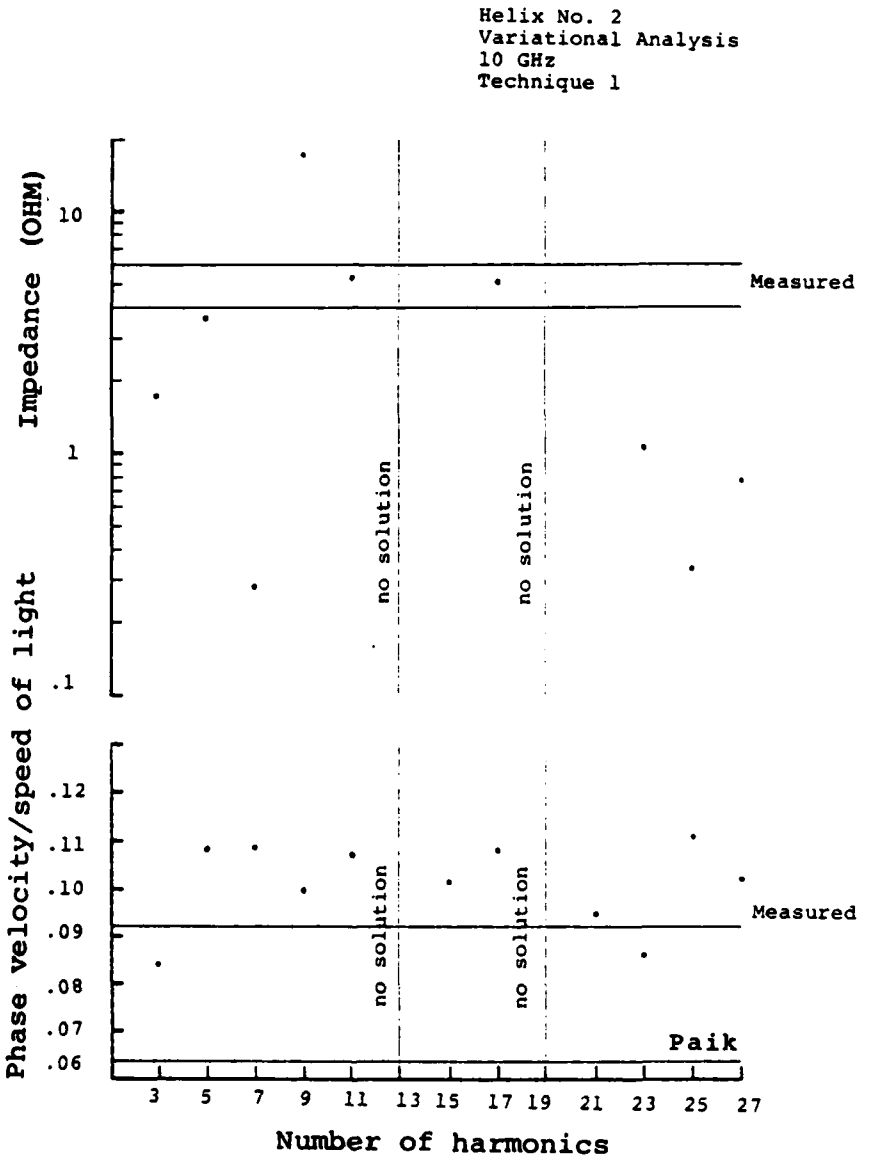

Figure 19. Trends in line impedance phase velocity as the number of trial fields increases on composite Helix No. 2.

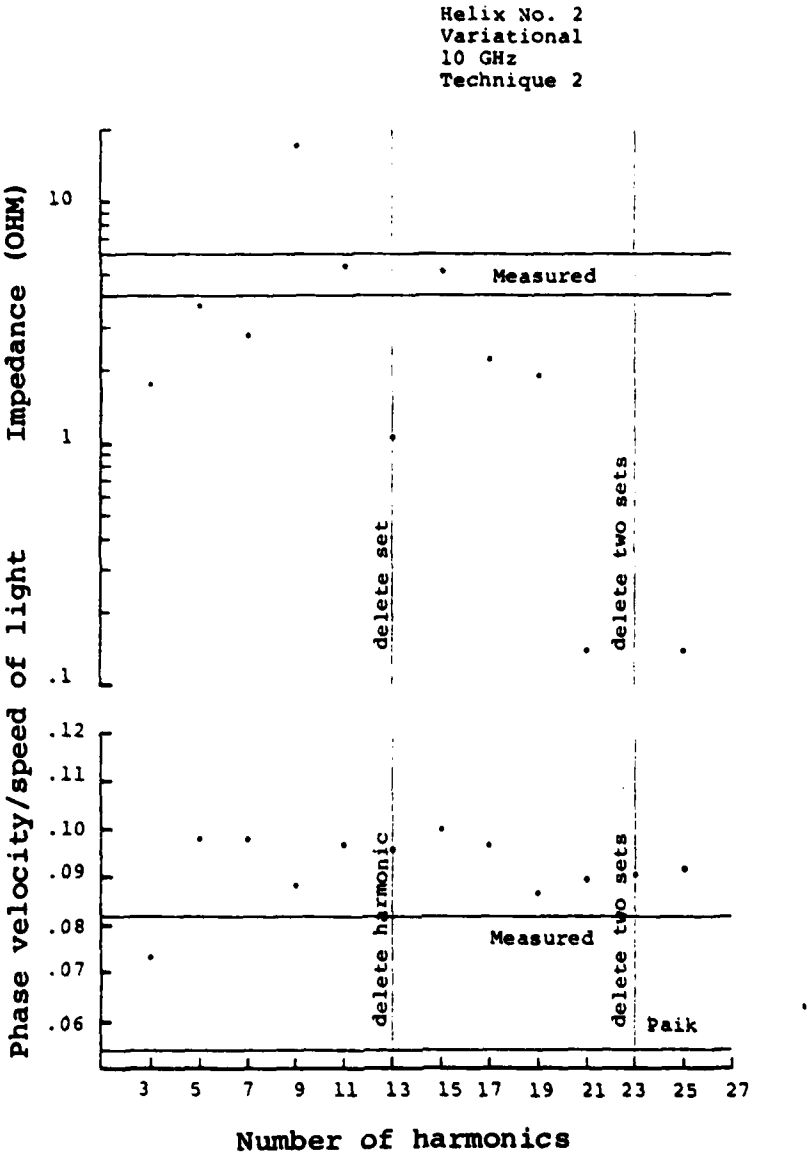

Figure 20. Trends in line impedance and phase velocity when some harmonics are deleted and simulation for composite Helix No. 2.

dispersion calculations. Figure 21 shows the dispersion for Helix No. 2 over a large frequency band using 9 and 21 harmonics. As can be seen, the computed results are much better than Paik and fairly parallel to measured results when 21 modes were used.

Helix No. 4, which has a large gap-to-pitch ratio, was examined at one frequency. Results for phase velocity were again large compared with measurement. This case is mentioned because a main motivation in using three regions was a lack of agreement between measurement and simulation when the two-region variational analysis was applied to Helix No. 4.

Extensive simulation of structures provided by Hughes Electron Dynamics Division have also been made. These are particularly of interest because quantitative data of dispersion and impedance, as well as qualitative changes when the dimensions were perturbed, can be seen. Results are presented here with frequency and geometric parameters normalized.

Figure 22 shows convergence properties for one Hughes structure. The behavior is similar to that of the Northrop ceramic structure. In Figure 23, results over a wide frequency band are compared to experiment for 11, 19, and 23 harmonics combined. All combinations give results closer than Paik. For 23 harmonics, the computed dispersion is extremely close to the measured results as is shown in Figure 24, using a finer scale in phase velocity.

Hughes perturbed the axial tape thickness in their structures. When the gap-to-pitch ratio is increased from .38 to .61, the dielectric loading of the external media decreases. This has the effect in both experimental and calculated results of increasing the phase velocity. Figure 25 shows calculated and measured responses over an octave of frequency. Although

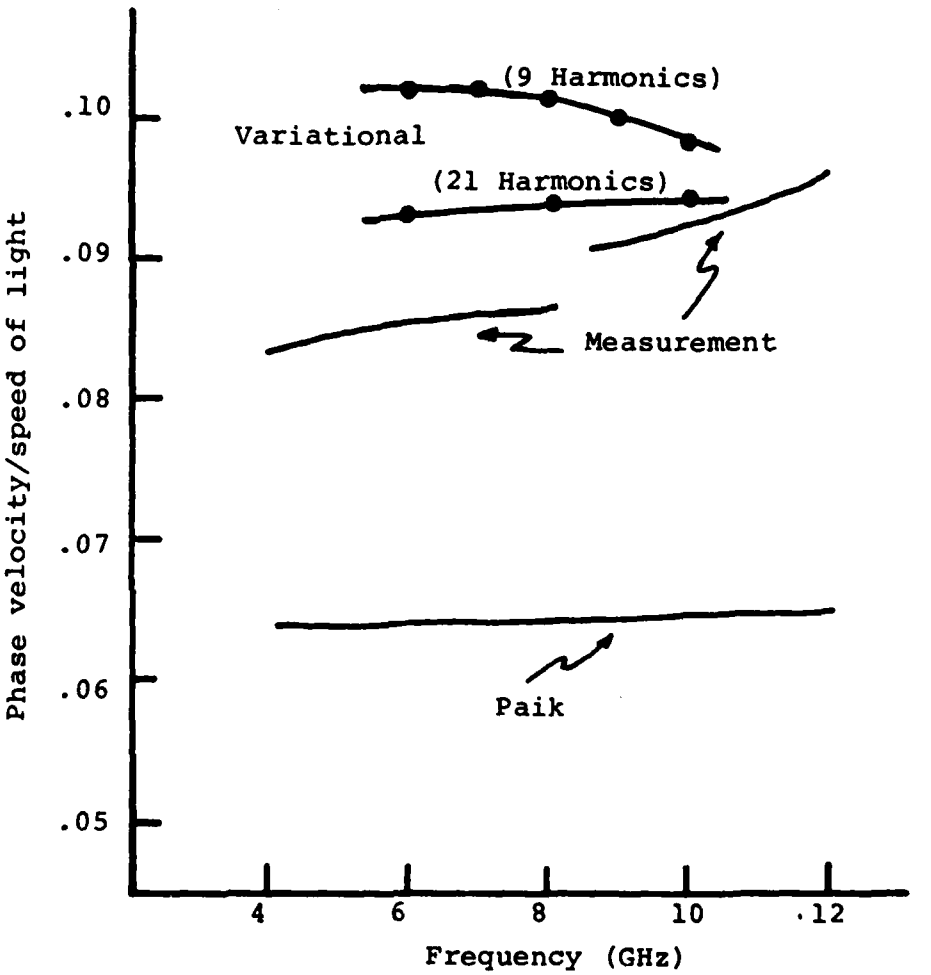

Figure 21. Comparisons between phase velocities from variational method, Paik theory and experiment for composite metal ceramic Helix No. 2.

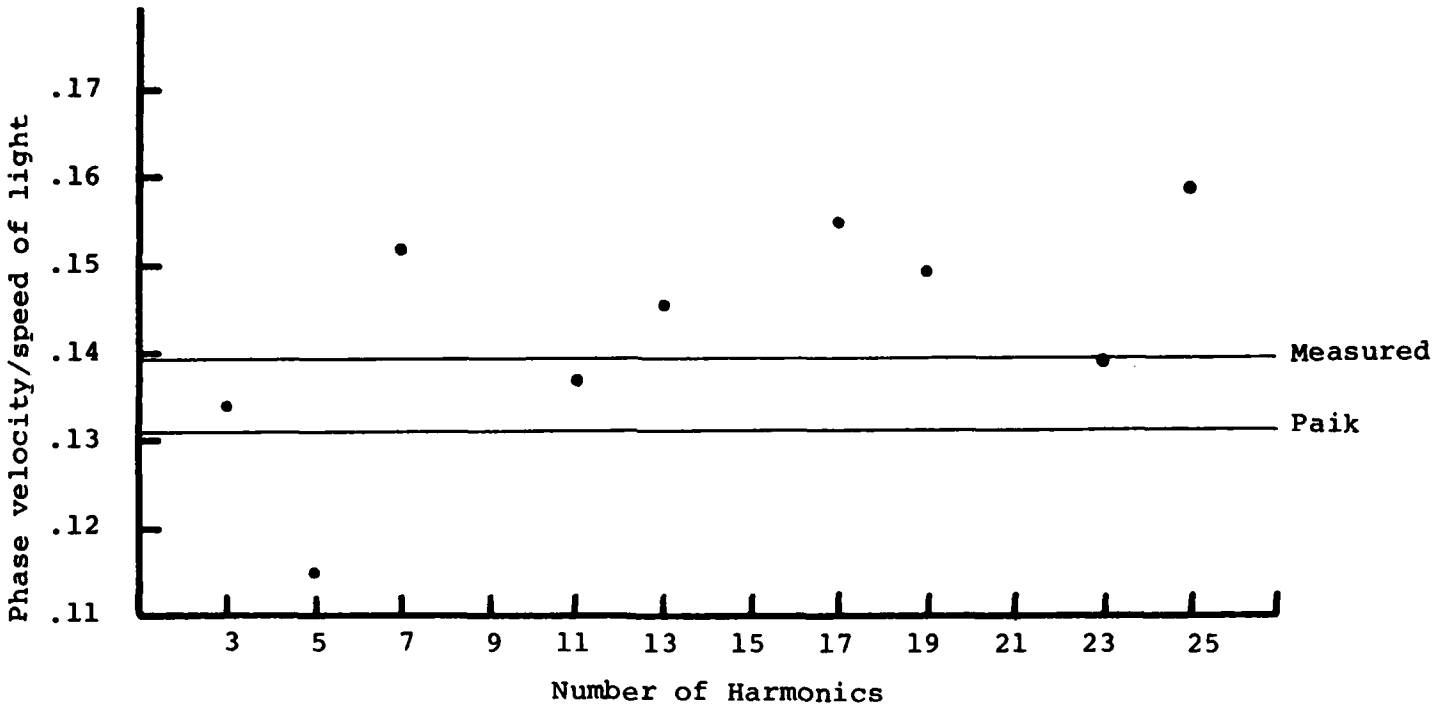

Figure 22. Trends in phase velocity vs.the number of trial field harmonics in simulation of Hughes composite Helix.

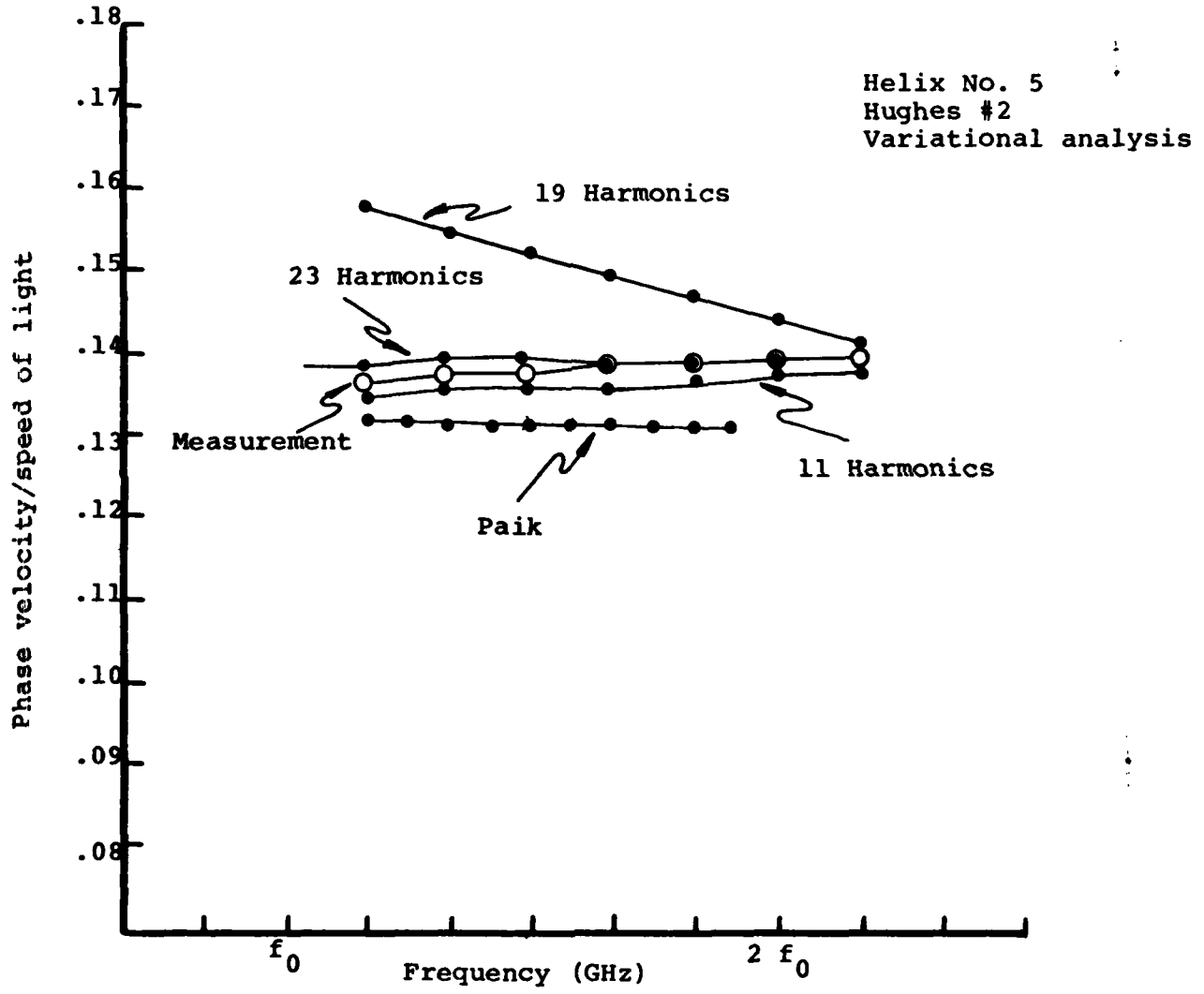

Figure 23. Comparison of phase velocity from variational method, Paik theory and experiment for Hughes composite metal ceramic Helix.

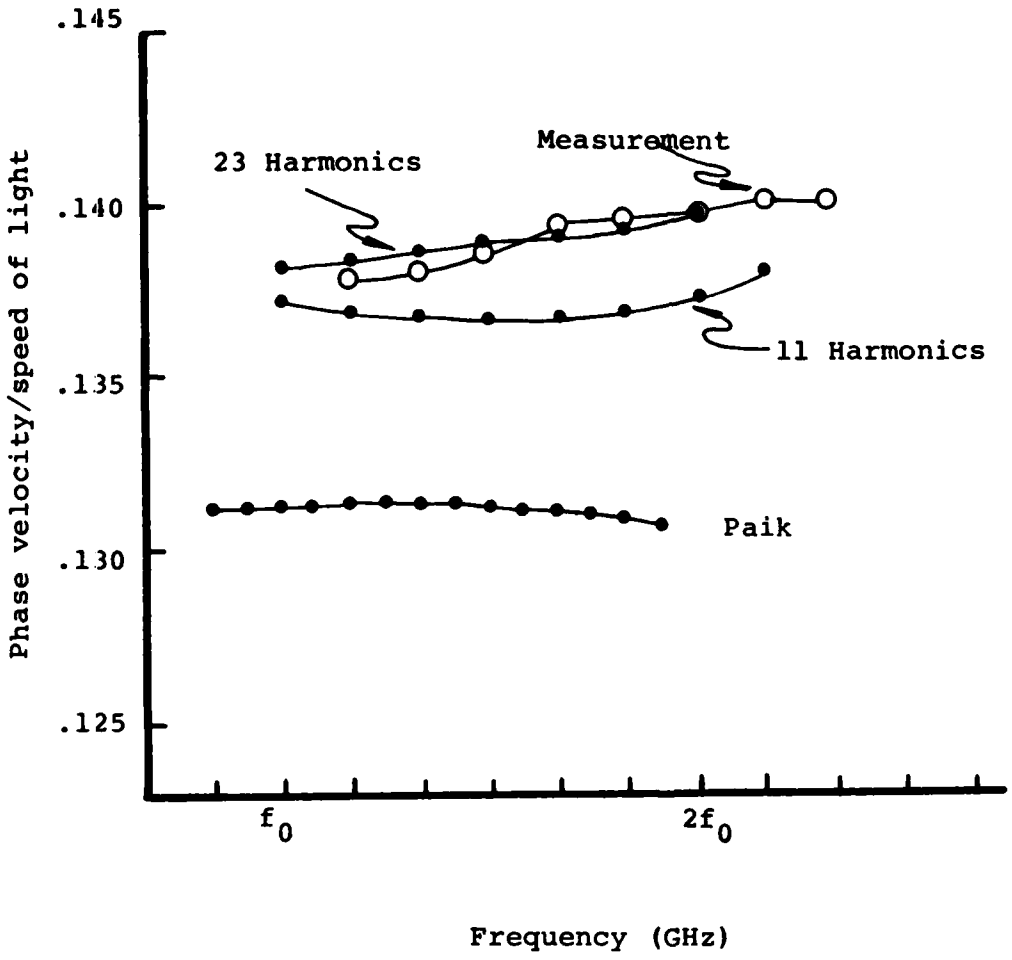

Figure 24. Comparison among phase velocities for Hughes ceramic helix using 23 harmonics.

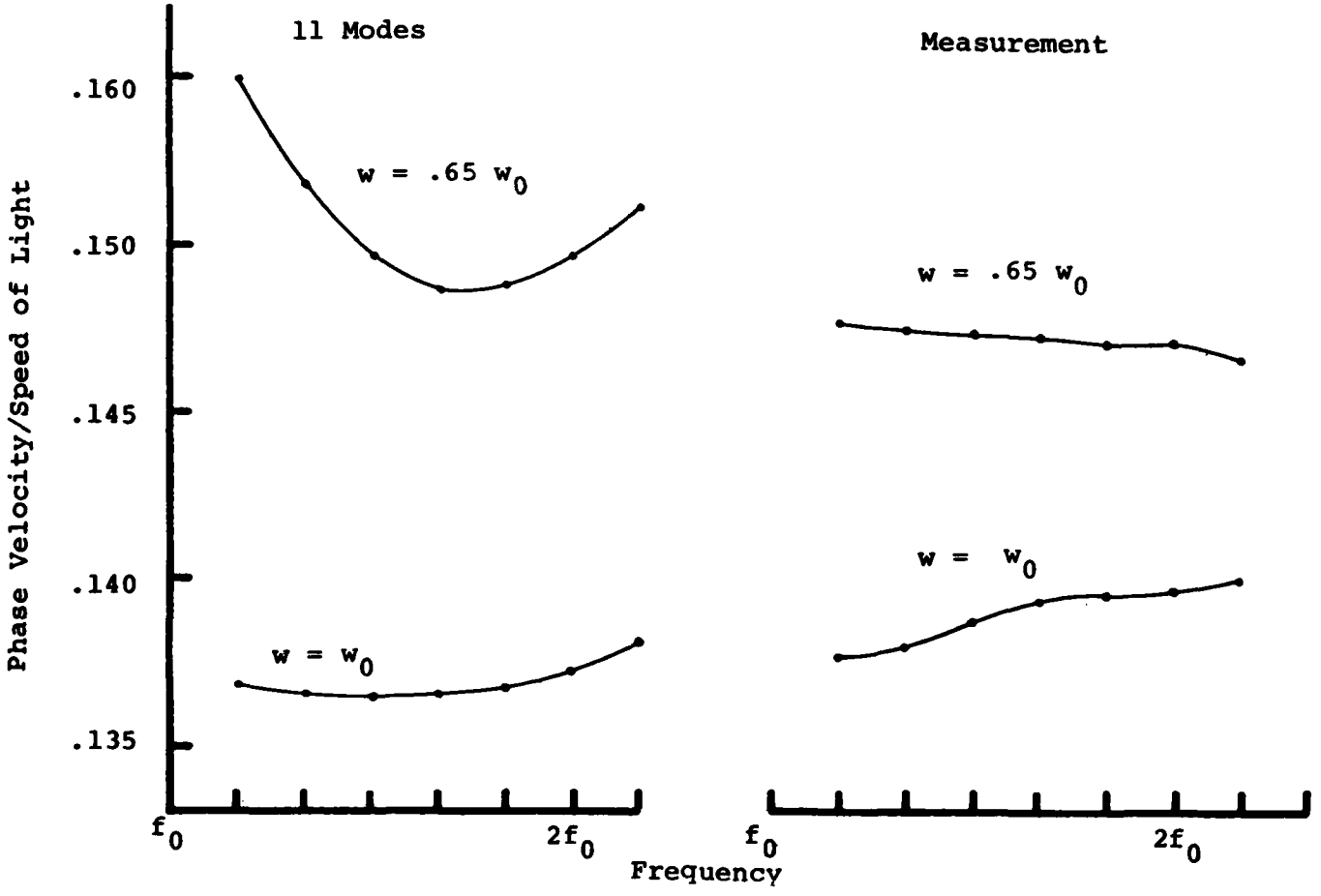

Figure 25. Comparison of dielectric loading effects from simulation and measurement for Hughes metal-ceramic helix.

simulation at 11 modes showed the increase in dispersion, the slope differs sharply from the calculated results.

Hughes also perturbed the shield diameter by increasing and decreasing this dimension by 10 percent. There are two opposing factors in such an experiment. By increasing the shield diameter, the phase velocity will tend to rise because the shield loading becomes close to that of a shieldless structure. At the same time, the effective dielectric loading is increased because more dielectric is contained in the external region. Shield loading is shown to dominate in this case as indicated in Figure 26. The computed dispersion from the three region variational analysis seems to be dominated by dielectric loading because the phase velocity has decreased with the increasing shield diameter. However, the movement is so slight that it is well within the present precision of the variational technique. It should be noted that predicted phase velocity remains nearly parallel to the measured dispersion.

We also examined other Northrop ceramic coated helices, though not in as much detail. Results for Helices No. 1 and 3 at three frequencies are shown in Figures 27 and 28 respectively.

C. Numerical Difficulties in Three Region Ceramic-Coated Helix Problems

By using three trial field regions instead of two, all actual geometric dimensions and dielectrics could be used without resorting to average or effective dimensions or dielectrics. At the same time, convergence properties, especially with regard to impedance, were sacrificed. Moreover, the dimension of the variation matrix grew rapidly with the number of trial field harmonics. This led to numerical instability in the calculation of the determinant of the matrix which was compounded

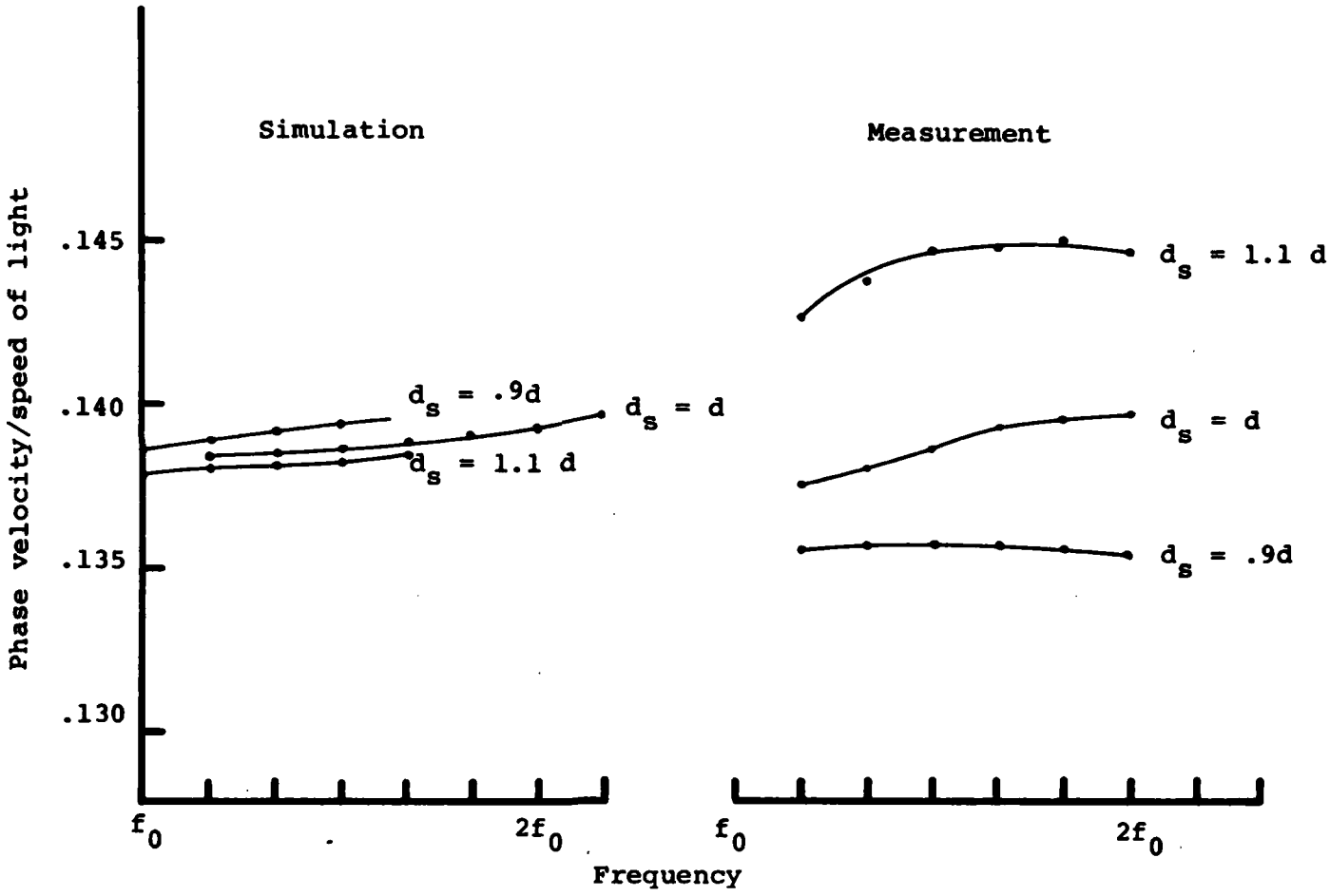

Figure 26. Comparison of shield loading effects from simulation and measurement for Hughes metal ceramic helix.

Frequency	No. of Harmonics
2 GHz	23
3.5 GHz	23
5 GHz	23

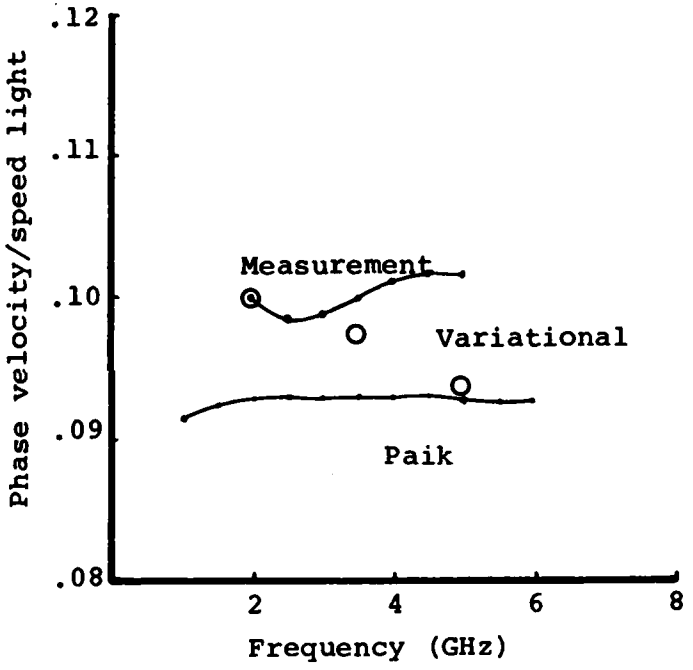

Figure 27. Comparison of phase velocities from variational analysis, Paik theory and experiment for composite Helix No. 1.

Frequency	No. of Harmonics
2 GHz	23
5 GHz	23
8 GHz	19

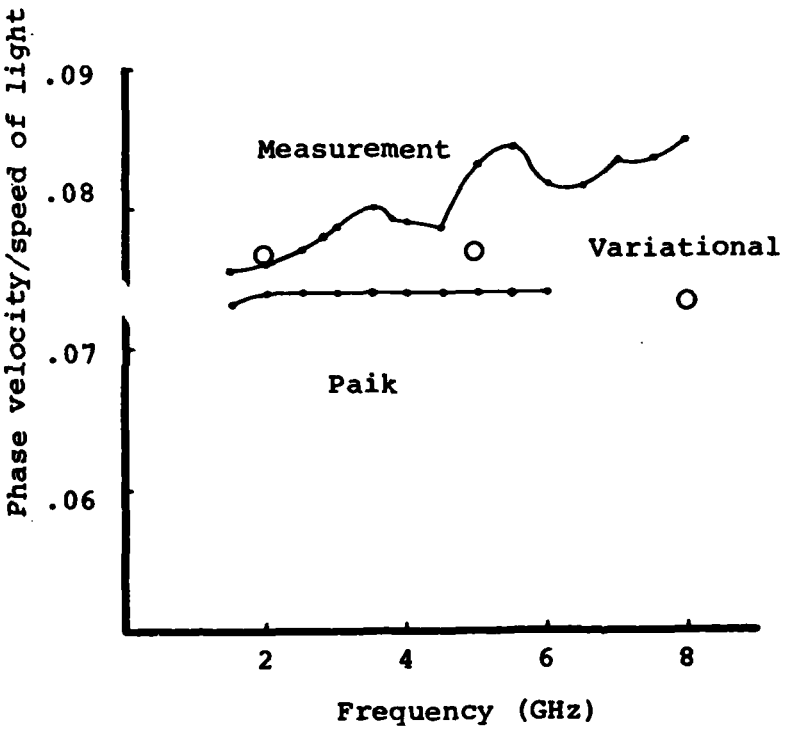

Figure 28. Comparison of phase velocities from variational analysis, Paik theory and experiment for composite Helix No. 3.

by perturbations introduced by imprecision in the numerical integration scheme for higher order modes.

Having six unknown fields per trial-field harmonic also introduced spurious solutions to the dispersion in much the same manner as four independent fields per harmonic affected the homogeneous support simulation. Our convention was to pick the smallest β_0. This may have been too arbitrary a convention.

Multiple solutions exist because in the variational technique the measure of equivalence of a sum of trial fields is their reaction with the correct currents in Rumsey's reaction integral. Two systems may have the same reaction even if they are not equivalent. Results suggest that introducing a great amount of freedom by supplying six trial fields per harmonic can produce several combinations of fields with equivalent reaction.

In the analysis of the homogeneous external support, two techniques were shown to remove false solutions to the variational analysis. Parallel developments have not been made for the spiralling support, and should be included in future work on the variational technique. The specific proposals are found in Section VIII.

Another main numerical instability was the determination of the singular matrix. The search routine favored situations in which the sign of the determinant changed. It is easy to miss singularities through which the sign of the determinant did not change. It is also easy to miss the smallest β_0 corresponding to a singular matrix if the sign changed more than once in an interval.

The amount of storage required for the three-region-spiral dielectric computer program (SPIRAL) is much greater than that

for the homogeneous case. When 13 angular harmonics are combined, 110K of fast memory are required. As noted previously, the CPU time used grows exponentially with the number of harmonics combined (see Figure 18).

SECTION VII

ERRORS INTRODUCED BY BEVENSEE'S CHOICE OF THE TRIAL FIELD

The fundamental approximation in the variational analysis is that the correct field can be written as a sum of cylindrical harmonics . Errors are introduced by (1) truncation of the series or (2) an inability to adequately represent the field with the cylindrical harmonics chosen. Expressing the exact system $\underline{c}$ as a sum of a truncated series of cylindrical modes, denoted by system $\underline{a}$ plus an error term $\varepsilon\underline{p}$ where the fields of $\underline{p}$ have norm equal to 1, yields

$$\underline{c} = \underline{a} + \varepsilon\underline{p} \quad . \tag{1}$$

If an arbitrary sum of modes is given by system $\underline{b}$, Equation 31(III) implies that

$$0 = \langle \underline{b}, \underline{a}^* \rangle + \varepsilon \langle \underline{b}, \underline{p}^* \rangle \quad . \tag{2}$$

The first term in 2 is just the quadratic form $B^{\dagger}M(\beta_0)C$ of Equation 25(III), when B and C are column vectors of coefficients of the cylindrical modes.

Clearly if $\varepsilon = 0$, then $\det[M(\beta_0)] = 0$. The fields produced by the sheath current problem fall into this category because the fields are indeed an exact sum of Bevensee's trial fields. It should be noted that our computer program quickly and correctly found the propagation constant for this case. Otherwise ε should be very small for some optimal combination of trial field harmonics. The case det(M) = 0, implies that the

reaction is zero for any b. However, ε may be large if the reaction $\langle b,p^* \rangle$ is zero for any b.

The fundamental assumption is the existence of a combination of trial fields which make ε so small that $M(\beta_0)$ can be considered singular. Bevensee's representation of the trial field is actually a decomposition into spiralling angular harmonics in terms of TE and TM longitudinal components:

$$\begin{bmatrix} E_z \\ H_z \end{bmatrix} = \quad = e^{-j\beta_0} \sum \begin{bmatrix} C_{1n} R_n(\gamma) \\ C_{2n} S_n(\gamma) \end{bmatrix} e^{jn\psi} \quad , \qquad (3)$$

where R and S_n are modified Bessel functions, $C_1 n$ are the constants of each of the trial field components and ψ is an angle which rotates with the helix. The functions $e^{jn\psi}$ are a complete basis as are the modified Bessel functions. However, Bevensee fixes n=m in order to make each individual trial field a solution to Maxwell's equations. It is our contention that this is too severe a restriction of the trial fields. The simple product of exponential and Bessel functions is not complete over the r-ψ surface.

The boundary conditions are violated by the trial function simultaneously across the tape radius and constant angles, ψ. For a given n, E_{Zn} and H_{Zn} cannot simultaneously be made continuous. This means that the continuity of the H-field across the tape radius and the condition of a zero tangential E-field along the tape radius must both be satisfied by higher harmonics. Notice the E-field problem is only along ψ, while the H-field discontinuity is only across a constant radius. In our variational solutions, many modes are needed primarily because the E-field problem and H-field problem compete. The following section

describes a planned modification which should allow continuity of the H-field and decrease the number of harmonics needed, thereby making the variational technique much more economical.

SECTION VIII

SUGGESTIONS FOR FUTURE WORK

A. Alternate Trial Fields

Additional terms should be added to the Bevensee's set of trial fields so that the collection is complete. Specifically express the longitudinal fields in each trial region as the sum in n and m of functions

$$\begin{bmatrix} E_Z \\ H_Z \end{bmatrix} = e^{-j\beta_0} \sum_{n=0}^{N} \sum_{m=0}^{M} \begin{matrix} C_{1nm} R_m(\beta_n Z) e^{-jn\psi} \\ C_{2nm} S_m(\beta_n Z) e^{-jn\psi} \end{matrix} , \quad (1)$$

where R_m, S_m, β_n, ψ are described in Section III. For (n=m), both E_Z and H_Z satisfy Maxwell's equation. This is the subset Bevensee used because only surface integrals remain in the variational formula for simple problems.

When $n \neq m$, volume integrals arise in Bevensee's formula. Equivalently, in Rumsey's reaction integral, volume magnetic and electric currents are added to the trial fields so that Maxwell's are satisfied.[10] These must be integrated over the volume of the structure.

The trial fields of Equation 1 have sufficient freedom to satisfy both E-field and H-field mismatches simultaneously. Also, minor modifications of the program architecture will be needed. In this way, it is anticipated that fewer angular harmonics will be needed in the approximate field because at a given angular harmonic, continuity of the longitudinal component of the E-field at the tape will not create a discontinuity in the H-field.

Because nearly correct boundary values in both E and H fields are possible with an optimal combination of trial fields, the number of spurious solutions should diminish too.

B. Reduction of Trial Field Harmonics by Point Matching

The existence of multiple solutions to the propagation constant for the homogeneous dielectric support problem was reduced by adding constraints from the continuity of the E-field across the tape radius. This reduced the number of unknown coefficients. These constraints do not exist for each harmonic for the spiral dielectric problem. However, continuity can be enforced at selected points along a particular interface on the total field. The number of independent trial field coefficients will then be reduced by four at each point where all boundary conditions are enforced.

This method is similar to point matching,[14] wherein sums of modes are placed in different sections of a structure and then matched along the interface of the partitions. Point matching typically uses all the unknown field coefficients to generate a matrix singularity at the propagation constant. It is usually successfully used when the structure has a large amount of symmetry.[15]

In the method proposed here, the variational expression would still be used, but the total trial field would be constrained at certain points. Results should be superior to those of of pure point matching because a solution to the variational expression has the correct reaction. Also, the interfaces are much more drastic than commonly encountered with point matching.

C. Use of Other Variational Expressions on the Spiral Dielectric

Results for the homogeneous dielectric drastically improved when an additional variational term was placed over the free-space region. Characterization of this term as weighing the free-space portion of the problem more heavily was made. No attempt has been made to add similar terms in the spiral dielectric simulation because additional numerical integrations would be required. Nevertheless, it is likely that the occurence of multiple solutions could be minimized by this technique on the spiral dielectric.

SECTION IX

CONCLUSIONS

Harris SAI has developed a variational analysis of several helical slow-wave structures. The formula of Bevensee was used. This was shown to be a measure of the reaction of the approximate field with the correct currents as defined by Rumsey. Through this reaction concept, effects of using an approximate sum of trial fields were derived.

The variational analysis of the sheath helix gives the exact phase velocity and trial function coefficients. When the variational analysis is applied to the homogeneous dielectric support, multiple solutions to the phase velocity appear. These are eliminated by either adding a variational term to Bevensee's formula or else reducing the number of unknown trial coefficients by applying constraints at the interface of trial regions. Results of phase velocity and impedance are extremely close to those found by a Paik analysis when the gap-to-pitch ratio is small.

The variational analysis was also applied to a spiraling dielectric support. If two trial regions were used, the results were too sensitive to the dielectric of the external trial region. A three-region analysis with thick tape was developed so that the complete geometry and all dielectrics were included in the model. Results were compared to cold-test data supplied by Northrop and Hughes. Multiple solutions again appeared. The lowest solution for β_0 changed greatly with different combinations of modes, as did the impedance. Nevertheless, there were combinations of trial function harmonics for which excellent agreement between simulation and experiment over a wide frequency range was observed.

The results suggest that more work should be done on the modeling of the spiral dielectric support. As described in Section VIII, it is suggested that a new set of trial fields and continuity constraints to minimize the occurrence of multiple β_0's be accomplished. Considerable improvement in the accuracy and economy of the variational model is expected. A viable solution to the spiral dielectric support can be extended quickly to cases using alternative support structures.

REFERENCES

1. J. R. Pierce, Traveling-Wave Tubes, Van Nostrand, Inc., New York; 1950.

2. D. A. Watkins, Topics In Electromagnetic Theory, John Wiley & Sons, Inc.,New York; 1958.

3. S. Sensiper, "Electromagnetic Wave Propagation on Helical Structures," Proc. IRE, vol. 43, No. 2, pp. 149-161; February 1955.

4. B. J. McMurtry, "Fundamental Interaction Impedance of a Helix Surrounded by a Dielectric and a Metal Shield," IRE Trans. on Electron Devices, vol. 9, No. 2, pp. 210-216; March 1962.

5. S. F. Paik, "Design Formulas for Helix Dispersion Shaping," IEEE Trans. on Electron Devices, vol. ED-16, No. 12, pp. 1010-1014; December 1969.

6. L. N. Loshakov and E. B. Ol'Derogge, "Propagation of Slow Electromagnetic Waves Along a Helix with Dielectric Supports," Radio Engineering and Electronic Physics, vol. 13, pp. 45-51; January 1968.

7. R. M. Bevensee, Electromagnetic Slow-Wave Systems, John Wiley & Sons, Inc.,New York; 1964.

8. D. A. Watkins and E. A. Ash, "The Helix as a Backward-Wave Circuit Structure," J. Appl. Phys., vol. 25, No. 6, pp. 782-790; June 1954.

9. D. M. MacGregor and J. E. Rowe, "Dual Mode TWT Design Studies," Tech. Report AFAL-TR-74-349, Air Force Avionics Laboratory, Wright-Patterson Air Force Base, OH; January 1975.

10. V. H. Rumsey, "The Reaction Concept in Electromagnetic Theory," Phys. Rev., ser. 2, vol. 94, No. 6, pp. 1483-1491; June 1954.

11. P. M. Morse and H. Feshbach, Methods of Theoretical Physics, vol. I, McGraw-Hill, New York; 1953.

12. R. F. Harrington, Time Harmonic Electromagnetic Fields, McGraw-Hill, New York; 1961.

13. R. E. Russel and O. F. Doehler, "Composite Metal Ceramic Helices," Final Technical Report, AFAL-TR-77-206.

14. J. E. Goell, "A Circular-Harmonic Computer Analysis of Rectangular Dielectric Wave Guides," Bell Syst. Tech. J., vol. 48, pp. 2135-2160; September 1969.

15. E. Yamashita, K. Atsuki, O. Hashimoto, and K. Kamijo, "Model Analysis of Homogeneous Optical Fibers with Deformed Boundaries," IEEE Trans. Microwave Theory Tech., vol. MTT-27, pp. 352-356; April 1979.

APPENDIX A

Data for a Northrop Corp. Metal-Ceramic Tape Helix

Manufacturer:

Northrop Corporation Defense Systems Division
175 W. Oakton Street
Des Plaines, IL 60018

Helix Identification Number: 1, 2, 3, and 4

Date Supplied To:

Dr. Donald M. MacGregor
Harris SAI, Inc.
611 Church Street
Ann Arbor, MI 48104
313/761-8612

A. For the helix and shield:

1. Material of tape: Copper
2. Electrical conductivity: 5.8×10^7 mho/meter
3. Material of shield: Aluminum
4. Electrical conductivity: 3.5×10^7 mho/meter
5. Inner radius of helix tape: (1)2.501, (2)0.9906,(3)1.35, (4)1.35 mm
6. Outer radius of helix tape: 2.769, 1.232,1.61,1.61 mm
7. Radius of conducting shield: 3.81, 1.613, 2.30, 2.30 mm
8. Pitch of helix tape: 2.489, 0.7874, 1.09, 2.27 mm
9. Width of the tape on the cylindrical surface, as measured at right angles to the spiral edge of the tape: 1.245, 0.51, 0.51, 0.51

B. For the dielectric support:

1. Material: Beryllium Oxide
2. Isotropic or anisotropic dielectric: Isotropic
3. Dielectric constants along principal axes: 6.7
4. Dielectric constant in radial direction:
5. Dielectric constant in angular direction:

C. Frequency Range

1. Low end of band: 2.0, 3.0, 1.4, 1.4 GHz
2. High end of band: 5.5, 12.0, 8.0, 8.0 GHz

D. Additional Information

The dielectric constant of beryllium oxide was supplied by Mr. Glenn Rees of Brush-Wellman, Inc., Elmore, Ohio. The remaining numbers are taken from Northrop Technical Report AFAL-TR-77-206, p. 34.[11]

MISSION
of
Rome Air Development Center

RADC plans and executes research, development, test and selected acquisition programs in support of Command, Control Communications and Intelligence (C^3I) activities. Technical and engineering support within areas of technical competence is provided to ESD Program Offices (POs) and other ESD elements. The principal technical mission areas are communications, electromagnetic guidance and control, surveillance of ground and aerospace objects, intelligence data collection and handling, information system technology, ionospheric propagation, solid state sciences, microwave physics and electronic reliability, maintainability and compatibility.

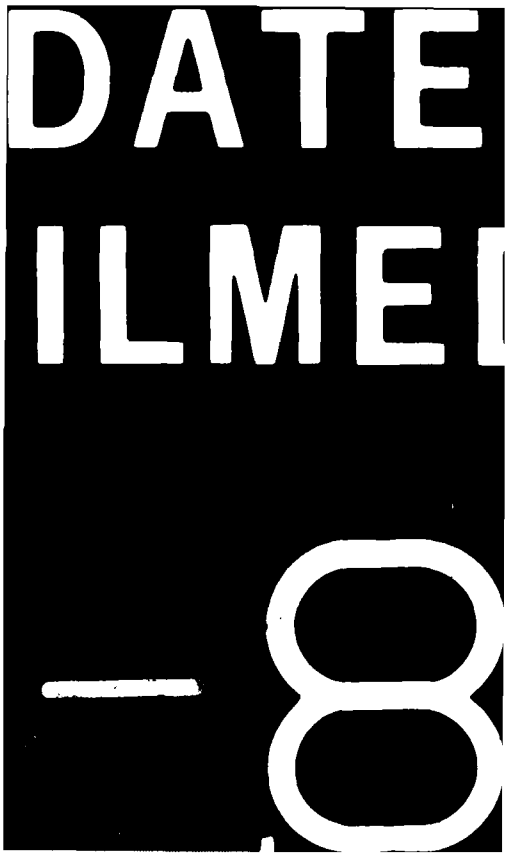
DATE
ILME
8